Strategies for simulating time evolution of Hamiltonian lattice field theories

Siddharth Hariprakash*,[1,2,3] Neel S. Modi*,[1,2] Michael Kreshchuk,[2] Christopher F. Kane,[4] and Christian W Bauer[2]

[1]*Center for Theoretical Physics and Department of Physics, University of California, Berkeley, California 94720, USA*
[2]*Physics Division, Lawrence Berkeley National Laboratory, Berkeley, California 94720, USA*
[3]*National Energy Research Scientific Computing Center (NERSC), Lawrence Berkeley National Laboratory, Berkeley, CA 94720, USA,*
[4]*Department of Physics, University of Arizona, Tucson, Arizona 85719, USA*

Simulating the time evolution of quantum field theories given some Hamiltonian H requires developing algorithms for implementing the unitary operator e^{-iHt}. A variety of techniques exist that accomplish this task, with the most common technique used in this field so far being Trotterization, which is a special case of the application of a product formula. However, other techniques exist that promise better asymptotic scaling in certain parameters of the theory being simulated, the most efficient of which are based on the concept of block encoding.

In this work we derive and compare the asymptotic complexities of several commonly used simulation techniques in application to Hamiltonian Lattice Field Theories (HLFTs). As an illustration, we apply them to the case of a scalar field theory discretized on a spatial lattice. We also propose two new types of block encodings for bosonic degrees of freedom. The first improves the approach based on the Linear Combination of Unitaries (LCU), while the second is based on the Quantum Eigenvalue Transformation for Unitary Matrices (QETU).

The paper includes a pedagogical review of utilized techniques, in particular Product Formulas, LCU, Qubitization, QSP, QETU, as well as a technique we call HHKL based on its inventors.

CONTENTS

* These authors contributed equally to this work.

I. INTRODUCTION

Performing precise numerical simulations is an essential ingredient in the studies of Quantum Field Theories (QFTs), which describe the most fundamental interactions within the Standard Model of particle physics. Some of the difficulties arising in such studies include: a large, non-conserving number of degrees of freedom; different types of particles and their interactions; and non-perturbativity of the strong interaction at large distances. A common approach to numerical simulation of field theories is provided by Euclidean Lattice field theory, where space-time is discretized and observables are calculated using the imaginary-time path integral formalism. For a recent overview of the field, see [1]. Such a conventional approach to lattice field theory relies on Monte-Carlo integration to perform the integral over the vast Hilbert space [2], which requires the weight of each field configuration to be real and positive. While this has been very successful, there are many observables for which Monte-Carlo integration is not possible due to the so-called sign problem [3, 4].

Many observables of interest, including dynamical ones, cannot be accessed through Monte-Carlo integration, and require calculations performed within the full Hilbert space. Such calculations are typically formulated in terms of Hamiltonian Lattice Field Theories (HLFT), in which space is discretized, while time is kept continuous [5–8].[2].

While resources required for the simulation of HLFTs on classical computers scale exponentially with the number of lattice sites [15], Jordan, Lee, and Preskill showed that quantum computers provide an exponential advantage over classical computers for this problem [16]. In fact, simulating QFT with the aid of quantum computers served as one of the motivations for the development of quantum computation [17], and is still considered as one of its most promising applications. For a recent review of the applications of quantum computing to high-energy physics, see [18].

A major task in such a scenario is the ability to efficiently simulate on a quantum computer the time evolution of a given Hamiltonian. In Ref. [19] Jordan, Lee, and Preskill made a detailed proposal to simulate a scalar field theory on quantum computers. Similarly to the earlier research [20–22], their work relies on the Suzuki-Trotter approximation [23–25] to compute the exponential of the Hamiltonian, and hence time evolve the scalar field theory. This is a specific example of a broader class of so called *Product Formulas* [24, 26] used for the task of time evolution [20, 27, 28].

This paper compares the resource requirements of various techniques to implement the time evolution operator of quantum field theories, considering Suzuki-Trotter approximations, nearly-optimal simulation strategies based on block encodings (BEs), as well as their combinations. We give the scaling for each method, with various parameters characterizing the problem at hand, such as the error allowed in the approximation of the evolution operator, the lattice size and other parameters of the Hamiltonian, as well as the time for which the system is evolved. This comparison is carried out for two very general classes of lattice Hamiltonians, but we also provide more detailed results for a scalar quantum field theory as an explicit example.

We provide two BE constructions for a bosonic degree of freedom, which outperform the general approach based on the Linear Combination of Unitaries (LCU) algorithm [29]. In the first case, we reduce the number of gates and ancillary qubits in the LCU algorithm by taking advantage of the quantum Fourier transform for switching between the eigenbases of the field and momentum operators. In the second case, we employ the Quantum Eigenvalue Transformation of Unitary Matrices (QETU) algorithm [30]; we find that while using QETU has a worse asymptotic complexity than using LCU combined with the Fourier transform, it requires less ancillary qubits.

We do not consider BEs based on the sparse oracle access input model, for two reasons. First, their construction is highly problem-specific [31–35]. Second, for local lattice field theories, which we consider as one of the major applications of the present work, our studies [35] indicate that the LCU-based approach is more efficient than that based the sparse oracle access.

A. Paper Structure

We start with setting up our notation in Sec. I B before presenting the main results of this paper in Sec. I C, with most of the information contained in Tables II to IV. In Sec. II we present a review of the various simulation algorithms. No new information is presented in this section, and the presentation is generic, not yet adapted for lattice field theory simulations. In Sec. III we use these algorithms to

[2] Note that while HLFTs sometimes refer solely to quantum field theories in the equal-time formulation, discretized on a spatial lattice [5, 6], in this work we assume (unless explicitly stated otherwise) a more general scenario which applies to any type of spatial discretization (e.g., spatial/momentum lattice [9] or any other single-particle basis set [10]), any type of field discretization (first or second quantization [9, 11]), as well as to both equal-time and light-front quantization [7, 8, 12–14].

give the scaling of the various techniques for the implementations of time evolution in lattice field theories. This will provide a derivation of the results presented in Sec. I C. In Sec. IV we present our results for a quartic scalar field theory. We discuss our results in Sec. V and conclude in Sec. VI.

B. Definitions and Notations used in this work

We begin by presenting the standard mathematical notation used to describe the asymptotic behavior of functions

Definition 1 (Asymptotic Notations)**.** Let $f, g : \mathbb{R} \to \mathbb{R}$ be functions of real variables. Then we say that $f = \mathcal{O}(g)$ if there exists a positive constant c such that $|f(x)| \leq c|g(x)|$ for all sufficiently large choices of x, i.e. $\forall x \geq x_0 \in \mathbb{R}$. We say that $f = \Omega(g)$ if $g = \mathcal{O}(f)$ and that $f = \Theta(g)$ if $f = \mathcal{O}(g)$ and $g = \mathcal{O}(f)$.

We see that $\mathcal{O}(\cdot)$ and $\Omega(\cdot)$ denote asymptotic upper and lower bounds respectively, while $\Theta(\cdot)$ denotes an asymptotically *tight* bound. We will make use of these notations throughout this work to denote the asymptotic scaling / behavior of of the variables we present in this section.

In HLFTs the degrees of freedom are typically the discretized quantum fields (in first quantization) or the eigenstates of the number operator (in second quantization) which live on the sites of a lattice.[3] For many Hamiltonians of interest, each term in the Hamiltonian couples fields belonging to a small subset of sites [5]. Depending on which fields get coupled together, one finds different types of Hamiltonians.

The first type of Hamiltonian we consider are of the form

$$\begin{gathered} H = \sum_{J \in S} H_J \,, \\ J = \{j_1, \ldots, j_{\mathsf{k}}\} \in S \,, \quad j_i \in \Lambda \,, \end{gathered} \tag{1}$$

where each each H_J acts nontrivially only on at most k sites j_i, labeled by $J = \{j_1, \ldots, j_{\mathsf{k}}\}$. Each lattice site is comprised of $\mathsf{n_q}$ qubits, each term H_J acts on $\mathsf{k}\mathsf{n_q}$ qubits, and the total system contains $\mathsf{n} = \mathsf{N_\Lambda}\mathsf{n_q}$ qubits.[4] The cardinality of the set S in Definition 2, which contains sets of indices used to label individual terms H_J, is also the total number of individual terms (denoted by $\mathsf{N_H}$) that form the full Hamiltonian H. We assume that in general, for a k-site-local Hamiltonian, the following scaling relation holds:

$$\mathsf{N_H} \equiv |S| = \mathcal{O}(\mathsf{N_\Lambda}^{\mathsf{m}}) \,, \tag{2}$$

where $\mathsf{m} \left(\in \mathbb{R}_{\geq 0}\right) \leq \mathsf{k}$ is parameter fixed by the choice of a specific theory.

We note that each summand H_J can be expressed in the Pauli basis as follows:

$$H_J = \sum_{i \in [\mathsf{N_P}^{(J)}]} c_i^{(J)} P_i^{(J)} \,, \tag{3}$$

where each $P_i^{(J)} \in \mathbb{C}^{2^{\mathsf{n}} \times 2^{\mathsf{n}}}$ represents an n-qubit Pauli operator, each $c_i^{(J)} \in \mathbb{C} \setminus \{0\}$ is a complex coefficient, and $\mathsf{N_P}^{(J)}$ enumerates the number of terms with non-zero coefficient in the Pauli decomposition of H_J. We introduce the quantity $\mathsf{N_P}$ as the maximum number of Pauli strings appearing in the decomposition of any single term H_J. We define it as follows:

$$\mathsf{N_P} \equiv \max_J \left(\mathsf{N_P}^{(J)}\right) . \tag{4}$$

In this way, the number of total Pauli strings appearing in a Hamiltonian with $\mathsf{N_H}$ summands can be bounded by $\mathsf{N_H}\mathsf{N_P}$. Note that for a k-site-local Hamiltonian $\mathsf{N_P} = \mathcal{O}(4^{\mathsf{k}n_q})$ always holds as an upper bound.

An important quantity in asymptotic gate complexity estimates is the 1-norm of a Hamiltonian H, denoted by $\|H\|_1$, and defined as

$$\|H\|_1 \equiv \sum_{J \in S} \|H_J\| \,, \tag{5}$$

where $\|\cdot\|$ represents the spectral / operator norm. The *induced* 1-norm of the Hamiltonian, denoted by $|||H|||_1$, can then be defined by maximizing the following sum over the qubit-index (within the multi-index variable $J \in S$) $\ell \in \{1, \ldots, k\}$ and the site-index $j_\ell \in \Lambda$:

$$\begin{gathered} |||H|||_1 \equiv \max_\ell \max_{j_\ell} \sum_{J_\ell^{(j_\ell)} \in S_\ell^{(j_\ell)}} \|H_J\| \,, \\ J_\ell^{(j_\ell)} = \{j_1, \ldots, j_{\ell-1}, j_{\ell+1}, \ldots, j_{\mathsf{k}}\} \in S_\ell^{(j_\ell)} \,, \\ J = \{j_1, \ldots, j_{\ell-1}, j_\ell, j_{\ell+1}, \ldots, j_{\mathsf{k}}\} \in S \,. \quad j_i \in \Lambda \,. \end{gathered} \tag{6}$$

[3] In some cases, the lattice is naturally embedded into some metric space, e.g., when a lattice in real or momentum space is used. More generally, it can be considered as the space which the index enumerating the degrees of freedom belongs to. Furthermore, we use the term "lattice site" for any local ingredient of the lattice that can support a Hilbert space. While for fermions and scalar fields these are the actual lattice sites, for gauge fields this terminology also covers the links and plaquettes of the lattice.

[4] We note that our definition of k-site-local Hamiltonian reduces to the usual definition of a k-local Hamiltonian on n-qubits [28] if we set $\mathsf{n_q} = 1$ and $\Lambda = \{1, 2, \ldots, \mathsf{n}\}$, in which case $\mathsf{N_H} \sim \mathsf{n}^{\mathsf{k}}$ and $\mathsf{N_P} \sim 4^{\mathsf{k}}$.

In other words, the induced 1-norm performs the sum over the norms $\|H_J\|$ which have the lattice site j_ℓ at the ℓ'th position and maximizes over all choices of ℓ and j_ℓ. This induced norm provides an upper bound on the *strength* of the Hamiltonian at any single site, such that the qubit-index of that site within the multi-index variable $J \in S$ is fixed, due to interactions with the remaining (allowed by locality restrictions and the specific theory under consideration) sites in the lattice. We denote by $\mathsf{N}_{\mathsf{ind}}$ the number of terms in the sum appearing in Eq. (6):

$$\begin{aligned} \mathsf{N}_{\mathsf{ind}} &\equiv |S_{\ell^*}^{(j_{\ell^*})}| \,, \\ \ell^*, j_{\ell^*} &= \underset{\ell}{\operatorname{argmax}} \underset{j_\ell}{\operatorname{argmax}} \sum_{J_\ell^{(j_\ell)} \in S_\ell^{(j_\ell)}} \|H_J\|, \end{aligned} \tag{7}$$

For general k-site-local Hamiltonians as defined in Definition 2 below, one finds

$$\mathsf{N}_{\mathsf{ind}} = \mathcal{O}\big(\mathsf{N}_\Lambda{}^{\mathsf{m}_{\mathsf{ind}}}\big) \,, \tag{8}$$

where $\mathsf{m}_{\mathsf{ind}}$ $(\in \mathbb{R}_{\geq 0}) \leq \mathsf{k} - 1$ is again a parameter fixed by the choice of a specific theory. We also define a quantity $\mathsf{c}_\mathsf{P} \in \mathbb{R}$ to be the maximum absolute value of the individual coefficients in the expansion of each H_J in terms of Pauli operators. Writing each summand H_J as in Eq. (3), we have that

$$\mathsf{c}_\mathsf{P} \equiv \max_{J,i} \{|c_i^{(J)}|\} \,, \tag{9}$$

so that $\|H\|_1 \leq \mathsf{c}_\mathsf{P}\mathsf{N}_\mathsf{P}\mathsf{N}_\mathsf{H}$ and $|||H|||_1 \leq \mathsf{c}_\mathsf{P}\mathsf{N}_\mathsf{P}\mathsf{N}_{\mathsf{ind}}$.

We define the *exponentiation error* ε as the difference between the exact time evolution operator e^{-iHt} and an approximate implementation $U(t)$

$$\varepsilon \equiv \|U(t) - \mathrm{e}^{-iHt}\| \,. \tag{10}$$

We note the functions we consider in this paper depend on ε only through the quantity $1/\varepsilon$. Thus our presentation of asymptotic notations (see Def. 1) is sufficient to study the behavior of such functions for asymptotically small values of ε.

We summarize these results in a few definitions, that will be used throughout this paper

Definition 2 (Site-local lattice Hamiltonian)**.** *A* k*-site-local Hamiltonian on a lattice* Λ *of size* $\mathsf{N}_\Lambda = |\Lambda|$ *is one of the form:*

$$\begin{aligned} H &= \sum_{J \in S} H_J \,, \\ J &= \{j_1, \ldots, j_\mathsf{k}\} \in S \,, \quad j_i \in \Lambda \,, \end{aligned} \tag{11}$$

where the number of terms in the set S *are given by* N_H*, each each* H_J *acts nontrivially only on at most* k *sites* j_i*, labeled by* $J = \{j_1, \ldots, j_\mathsf{k}\}$*, and each lattice site is comprised of* n_q *qubits. Let each term* H_J *take the form* (3) *and, as in* (4)*, let* N_P *be an upper bound on the number of distinct Pauli strings appearing in the decomposition of any single term* H_J*. Let* c_P *be the largest magnitude of any Pauli coefficient over all terms as in* (9)*, and* $\mathsf{N}_{\mathsf{ind}}$ *be the number of terms in the induced 1-norm of the Hamiltonian as in Eq.* (7)*.*

Many HLFT Hamiltonians have the property that they only couple fields at neighboring lattice locations together, giving rise to a *geometric* locality. Defining a distance metric to the different lattice sites, allows to define a k-geometrically-site-local Hamiltonian, which is a sum of operators, each involving only sites belonging to a connected set.

Definition 3 (Geometrically-site-local lattice Hamiltonian)**.** *A* k*-geometrically-site-local lattice Hamiltonian is a* k*-site-local lattice of Hamiltonian in which each individual term* H_J *acts on a connected set of sites* J*.*[5]

The restriction of geometric locality implies that each term H_J acts upon belong to a ball of diameter k, which imposes a tighter bound on $\mathsf{N}_{\mathsf{ind}}$:[6]

$$\mathsf{N}_{\mathsf{ind}} \leq \binom{\mathsf{k}^\mathsf{d}}{\mathsf{k}} = \mathcal{O}(1) \,, \tag{12}$$

i.e., $\mathsf{N}_{\mathsf{ind}}$ no longer scales with N_Λ (note here that have assumed a constant value for the spatial dimension d). Furthermore, since each set J can be labeled by the center of the corresponding ball, the number of sets and hence terms in the Hamiltonian is given by

$$\mathsf{N}_\mathsf{H} = \mathcal{O}(\mathsf{N}_\Lambda) \,. \tag{13}$$

Hamiltonians of relativistic quantum field theories typically depend on the values of fields and their derivatives at a given point, thus one can expect that lattice formulations of these theories exist such that they are geometrically local. This is the case for the scalar field theory considered later in this paper for example. For gauge theories, gauge invariance needs to be included into the considerations, and the locality of the Hamiltonian now depends on what basis is chosen for the fields. In so-called electric bases, Gauss's law constraints are still local, such that the

[5] One typically assumes that the lattice is embedded into some metric space. In our work, we assume a hypercubic lattice with spacing 1. In principle, one could define locality without introducing a metric structure, e.g., by using a more general topology on S.

[6] The precise upper bound in Eq. (12) is given for a hypercubic lattice, but statement on independence of $\mathsf{N}_{\mathsf{ind}}$ on N_Λ is general.

Λ	Lattice
$\mathsf{N}_\Lambda = \lvert\Lambda\rvert$	Lattice size
J	Multi-index enumerating Hamiltonian terms
$H = \sum_{J\in S} H_J$	Hamiltonian
k	Hamiltonian site-locality
H_J	Term acting on k sites
S	Set containing sets of indices J
$\mathsf{N}_\mathsf{H} = \lvert S\rvert$	Number of summands forming H
n_q	Number of qubits per lattice site
$\mathsf{n} = \mathsf{N}_\Lambda \mathsf{n}_\mathsf{q}$	Total number of qubits
${\mathsf{N}_\mathsf{P}}^{(J)}$	Number of Pauli terms representing a single term H_J
N_P	$\max_J({\mathsf{N}_\mathsf{P}}^{(J)})$
c_P	Maximum Pauli coefficient in H
D	Hamiltonian geometric locality
d	Spatial dimension
d	Degree of Chebyshev polynomial
ε	Exponentiation error
m	Parameter describing the scaling of N_H with respect to N_Λ, see Eq. (2)
m_ind	Parameter describing the scaling of N_ind with respect to N_Λ, see Eq. (8)
χ	Total number of elementary gates

Table I. Notations used throughout the paper.

final Hamiltonian is geometrically local in this basis. On the contrary, magnetic bases, behaving better at small bare coupling (which is required in the continuum limit), require non-geometrically local interactions [36–41].

As we will also consider Hamiltonians that act only on $\mathcal{O}(1)$ number of lattice sites, we will also provide the definition for them:

Definition 4. [$\mathcal{O}(1)$ lattice Hamiltonian] *Let H be a ($\mathsf{k} = \mathsf{N}_\Lambda = \mathcal{O}(1)$)-site-local Hamiltonian, with N_P and c_P defined as in Eqs.* (4) *and* (9)*. Note that $\mathsf{N}_\Lambda = \mathcal{O}(1)$ also implies $\mathsf{N}_\mathsf{H} = \mathcal{O}(1)$, and that there is no difference between a site-local and geometrically site-local Hamiltonian in this case.*

C. Main results

The main results of this paper are summarized in Tables II to IV. Detailed derivations of these expressions will be given in Sec. III.

We first consider the results for a lattice containing $\mathcal{O}(1)$ sites, and compare the implementation of the time evolution operator after a Product Formula (PF) based splitting to the implementation using Quantum Signal processing (QSP). Both of those techniques will be introduced and defined in Sec. II. The important parameters that the time evolution operator depends on are the time t the system is evolved for, the number of Pauli terms N_P and maximum coefficient c_P in the Hamiltonian, as well as the exponentiation error ε. The scaling with these parameters is shown in Table II, where p denotes the order of the PF used. While the scaling of the PF implementation on all parameters improves as p is increased, the number of gates needed is typically exponential in p, so the order of the PF is typically chosen as $p = \mathcal{O}(1)$. One can therefore see that QSP has a better scaling than PFs in all parameters, with the most dramatic improvement being in the scaling in ε, which is exponentially better.

Next, we include the asymptotic scaling with the size of the lattice N_Λ for a k-site local Hamiltonian. The Hamiltonian is a sum of terms H_J, each of which acts on $\mathsf{k} = \mathcal{O}(1)$ lattice sites, and which in general do not commute with one another. One approach is to assemble the terms H_J using a PF, with the implementation of each H_J performed either using a PF or QSP, as just discussed. These two choices are compared in the first column of Table III. One can see that the scaling is more favorable in all parameters when the individual terms H_J are themselves implemented using a (different) PF.

A second approach is to use QSP for the entire Hamiltonian, with the corresponding scaling shown in the second column of Table III. One can see that this leads to worse scaling (in general) with the number of lattice sites than the PF, while giving a much better scaling with ε. Therefore, the usage of PF may be preferential in situations when $\mathsf{N}_\mathsf{H} \gg 1/\varepsilon$, which is often the case in field theory.

Local implementation	Complexity for $\mathcal{O}(1)$ sites
Product formula	$\mathcal{O}\Big[(\mathsf{N}_\mathsf{P})^{2+\frac{1}{p}}\,(\mathsf{c}_\mathsf{P} t)^{1+\frac{1}{p}}\,\varepsilon^{-\frac{1}{p}}\Big]$
QSP	$\mathcal{O}\Big[\mathsf{N}_\mathsf{P}\log\mathsf{N}_\mathsf{P}\,\big(\mathsf{N}_\mathsf{P}\mathsf{c}_\mathsf{P} t + \log(1/\varepsilon)\big)\Big]$

Table II. Scaling of a Hamiltonian defined on $\mathcal{O}(1)$ lattice sites. The scaling is given in terms of the number of Pauli strings N_P of a single term in the Hamiltonian Eq. (4), the largest coefficient of each of these Pauli strings c_P Eq. (9), and the exponentiation error ε, defined in Eq. (10).

Finally, we consider the case of geometrically-local Hamiltonians. In this case one still has the same two possibilities for the implementation, shown in the first two columns of Table IV. Both have an improved scaling in the number of lattice sites N_Λ due to the geometric locality, and as before the QSP approach wins in terms of dependence on ε while the PF-based wins in terms of scaling with N_Λ. The geometric locality of the Hamiltonian, however, allows for the use of the HHKL algorithm, introduced in Sec. II C, to assemble the H_J terms, with each local term again implemented via either PF or QSP. The scaling of this approach is shown in the third column of Table IV. We can see that this leads to a better scaling in N_Λ, with a combination of HHKL with QSP leading to the best overall scaling. The scaling of course does not give any information on the prefactor, that could be considerably larger for HHKL than for product based approaches [27]. Furthermore, the scaling given here is not tight, so it could be that for realistic scenarios product based formulas still win. Note that the scaling of PFs is identical to that of HHKL combined with PFs.

As a case study, we consider a scalar lattice field theory and express the obtained asymptotic gate complexities in terms of model parameters. This requires specifying the BE used, and we consider three methods for constructing the BE subroutine U_H in the scalar lattice field theory. The (LCU) algorithm [29], efficiently accomplishes this task for arbitrary local Hamiltonians, and can be applied to the Hamiltonian H of the entire system. Two alternative approaches are presented, both of which we use fewer gates for constructing the BE U_{H_J} for each H_J term in H while the LCU procedure is used for combining the BEs U_{H_J} into U_H. The first approach employs the Fourier Transform for switching between the eigenbases of position and momentum operators, which exponentially improves the asymptotic cost of U_{H_J} in terms of the number of qubits $\mathsf{n_q}$ per site. The second approach constructs U_{H_J} using the QETU algorithm [30, 42]. Despite worse asymptotic scaling, for a small number of qubits the QETU construction leads to gate costs similar to those in the previous approach yet only requires a single ancillary qubit per U_{H_J}. The comparisons of costs for various approaches is shown in Fig. 8. Finally, we use the best available construction of BE in order to compare the gate counts between the PF and QSP approaches in application to a single site of the φ^4 theory, see Fig. 9.

II. REVIEW OF SIMULATION ALGORITHMS

In this section, we review some algorithms commonly used in the literature for simulating the time evolution of generic quantum systems. We will focus on algorithms based on Product Formulas (PFs) [27, 28] and Quantum Signal Processing (QSP) [43, 44], both of which can be applied to small and spatially extended systems. We also review the HHKL algorithm [45], which may serve as a "nearly-optimal wrapper" of local evolution operators in geometrically-local system. These algorithms will serve as the building blocks from which we express algorithms for Hamiltonian lattice field theories in later chapters.

The discussion in this section aims to be a standalone discussion that gives the reader a basic understanding of the different tools used to implement a time evolution operator. While we aim to make this section accessible to readers without much background in the topic, we will still provide a precise set of statements and theorems that will be used later. Note that this section is not detailed enough to rederive all of these results, and for this we refer the reader to the papers cited in this section.

Note also that this discussion is kept very general, without restricting ourselves to the Hamiltonians considered in this work (except when stated explicitly otherwise).

A. Product-formulas

We begin by considering a time-independent Hamiltonian

$$H = \sum_{\gamma=1}^{\Gamma} H_\gamma \tag{14}$$

comprised of Γ summands, such that one can efficiently construct quantum circuits to implement the exponential $\mathrm{e}^{-iH_\gamma t}$ of each summand appearing on the RHS of Eq. (14). The unitary operator (called the time evolution operator for H) given by the exponential e^{-iHt} describes evolution under the full Hamiltonian H for some arbitrary time t. PFs allow us to construct an approximation to the full time evolution operator by decomposing it into a product of exponentials, each involving a single summand. The general form of a PF (see Ref. [28]) is given by

$$\mathrm{e}^{-iHt} \approx S(t) = \prod_{\upsilon=1}^{\Upsilon} \mathcal{P}_\upsilon \left(\prod_{\gamma=1}^{\Gamma} \mathrm{e}^{-ita_{\upsilon,\gamma} H_J} \right), \tag{15}$$

such that each $a_{\upsilon\gamma} \in \mathbb{R}$ and $\sum_{\upsilon=1}^{\Upsilon} a_{\upsilon\gamma} = 1 \ \forall \gamma \in [\Gamma] \equiv \{1, 2, \ldots, \Gamma\}$. The latter condition ensures that each individual term H_γ is evolved for the total time t. The parameter Υ determines the total number of stages in the PF, and for each stage $\upsilon \in [\Upsilon]$ there exists a corresponding permutation operator $\mathcal{P}_\upsilon$ that determines the ordering of the individual exponentials within that stage (the specific actions of the operators $\mathcal{P}_\upsilon$ depend on the chosen PF construction). PFs of the form Eq. (15) provide good approximations to the full time evolution operator when the evolution time t is small, and in particular one defines a p^{th} order PF $S_p(t)$ as one that is correct up

Local implementation	Assembly using PF	QSP for entire system
Product formula	a) $\mathcal{O}\Big(\mathsf{N_{ind}}\mathsf{N_P}\left(\mathsf{N_H}\mathsf{N_P}\mathsf{c_P}t\right)^{1+\frac{1}{p}}\varepsilon^{-\frac{1}{p}}\Big)$	
QSP	b) $\mathcal{O}\Big[\mathsf{N_{ind}}\left(\mathsf{N_H}\mathsf{N_P}\mathsf{c_P}t\right)^{1+\frac{1}{p}}\varepsilon^{-\frac{1}{p}}\mathsf{N_P} \times \log\mathsf{N_P}\log(\mathsf{N_{ind}}\mathsf{N_H}\mathsf{N_P}\mathsf{c_P}t/\varepsilon)\Big]$	c) $\mathcal{O}\Big[\mathsf{N_H}\mathsf{N_P}\log(\mathsf{N_H}\mathsf{N_P})\left(\mathsf{N_H}\mathsf{N_P}\mathsf{c_P}t+\log(1/\varepsilon)\right)\Big]$

Table III. Resource scaling for site-local Hamiltonians as in Definition 2. The two rows label the local implementation for each term e^{-iH_Jt} either using a PF (top row) or using QSP (bottom row). The two columns show how the various terms H_J are combined together, either using a PF (left column) or doing the whole evolution using QSP (bottom right). Cases a), b), and c) are studied in Sec. III A 1, Sec. III C, and Sec. III B 1, correspondingly.

Local implementation	Assembly using PF	QSP for entire system	Assembly using HHKL
Product formula	d) $\mathcal{O}\Big(\mathsf{N_P}\left(\mathsf{N_\Lambda}\mathsf{N_P}\mathsf{c_P}t\right)^{1+\frac{1}{p}}\varepsilon^{-\frac{1}{p}}\Big)$		e) $\mathcal{O}\Big(\mathsf{N_P}\left(\mathsf{N_\Lambda}\mathsf{N_P}\mathsf{c_P}t\right)^{1+\frac{1}{p}}\varepsilon^{-\frac{1}{p}}\Big)$
QSP	f) $\mathcal{O}\Big[\left(\mathsf{N_\Lambda}\mathsf{N_P}\mathsf{c_P}t\right)^{1+\frac{1}{p}}\varepsilon^{-\frac{1}{p}}\mathsf{N_P} \times \log\mathsf{N_P}\log(\mathsf{N_\Lambda}\mathsf{N_P}\mathsf{c_P}t/\varepsilon)\Big]$	g) $\mathcal{O}\Big[\mathsf{N_\Lambda}\mathsf{N_P}\log(\mathsf{N_\Lambda}\mathsf{N_P}) \times \left(\mathsf{N_\Lambda}\mathsf{N_P}\mathsf{c_P}t+\log(1/\varepsilon)\right)\Big]$	h) $\mathcal{O}\Big[\mathsf{N_\Lambda}\mathsf{N_P}^2\mathsf{c_P}t\left[\log(\mathsf{N_\Lambda}t/\varepsilon)\right]^{\mathsf{d}} \times \log(\mathsf{N_P}\log(\mathsf{N_\Lambda}t/\varepsilon))\Big]$

Table IV. Resource scaling for geometrically site-local Hamiltonians as in Definition 2. The two rows label the local implementation for each term e^{-iH_Jt} either using a PF (top row) or using QSP (bottom row). The three columns show how the various terms H_J are combined together, either using a PF (left column), using the HHKL algorithm (right column), or doing the whole evolution using QSP (bottom middle). Cases d), f), and g) are obtained from cases a), b), and c), respectively, in Table III upon setting $\mathsf{N_H}=\mathcal{O}(\mathsf{N_\Lambda})$ and $\mathsf{N_{ind}}=\mathcal{O}(1)$. Cases e) and h) are studied in Sec. III D.

to p^{th} order in t

$$S_p(t)=\mathrm{e}^{-iHt}+\mathcal{O}(t^{p+1})\,. \tag{16}$$

The simplest example of a PF arises from the use of the Baker-Campbell-Hausdorff formula

$$\mathrm{e}^{A+B}=\mathrm{e}^{A}\mathrm{e}^{B}+\mathcal{O}([A,B])\,, \tag{17}$$

and thus we can write

$$\mathrm{e}^{-iHt}\approx S_1(t)=\prod_{\gamma=1}^{\Gamma}\mathrm{e}^{-iH_\gamma t}\,. \tag{18}$$

This approximation is known as the first order Lie-Trotter formula. The higher (even) order Suzuki-Trotter formulas are defined recursively as

$$\begin{aligned}S_2(t)&\coloneqq\prod_{i=1}^{\Gamma}\mathrm{e}^{\frac{-iH_it}{2}}\prod_{i=\Gamma}^{1}\mathrm{e}^{\frac{-iH_it}{2}}\,,\\ S_{2k}(t)&\coloneqq S_{2k-2}(u_kt)^2S_{2k-2}((1-4u_k)t)\\ &\qquad\times S_{2k-2}(u_kt)^2\,,\end{aligned} \tag{19}$$

where $u_k\equiv1/\left(4-4^{1/(2k-1)}\right)$, and the product given by $\prod_{i=\Gamma}^{1}(\cdot)$ corresponds to reversing the order in which we choose the variable i with respect to the first product given by $\prod_{i=1}^{\Gamma}(\cdot)$. In theory, one could use such a construction to build arbitrarily large order PFs. However the number of stages Υ, and hence the number of elementary gate operations required to construct a circuit implementing such a PF, grows exponentially with the order p (see Ref. [28]). For this reason, we use relatively low order formulas for practical applications and our results assume that $p,\Upsilon(p)=\mathcal{O}(1)$.

Since PFs have corrections that depend polynomially on the evolution time t, they give good approximations for small t. Given a PF valid for small t, however, we can obtain one for longer times. The general procedure is to divide the full evolution time t into r (known as the *Trotter number*) smaller time steps, and apply the chosen p^{th} order PF to each step, describing the evolution for a smaller time t/r, before multiplying together the results from the individual steps

$$S_p(t)=(S_p(t/r))^r, \tag{20}$$

and the associated exponentation error ε is given by

$$\varepsilon=\|(S_p(t/r))^r-\mathrm{e}^{-iHt}\|\,. \tag{21}$$

To work out the resource requirements to satisfy such an error bound, we ask for the required Trotter number r for a p^{th} order formula to satisfy Eq. (21) given a fixed value of ε. In general the answer depends on the asymptotic scaling on the evolution time t, as well as the norms of the individual summands H_γ and the commutators amongst them.

While Eq. (16) provides the correct asymptotic dependence of the error on t, Refs. [28] and [46] present bounds that show explicit dependence on the 1-norm of the full Hamiltonian (given by $\sum_{\gamma=1}^{\Gamma}\|H_\gamma\|$). Note however, that these bounds are not tight. For example, when all the summands H_γ commute, the exponentiation error ε becomes zero while these error bounds can become arbitrarily large. This was further addressed in Ref [28], where the authors present another (tighter) bound that results from exploiting the commutativity properties of the summands H_γ. This led to the following asymptotic scaling of the Trotter number

$$r = \mathcal{O}\left(\frac{\tilde{\alpha}^{\frac{1}{p}} t^{1+\frac{1}{p}}}{\varepsilon^{\frac{1}{p}}}\right), \tag{22}$$

where $\tilde{\alpha} \equiv \sum_{\gamma_1,\gamma_2,\ldots,\gamma_{p+1}=1}^{\Gamma} \||[H_{\gamma_{p+1}}, \ldots[H_{\gamma_2}, H_{\gamma_1}]]\||$.

Note that not every Trotter number r satisfying the asymptotic upper bound (22) will yield the desired error bound. Rather, the above result merely provides an asymptotic upper bound on the *minimum* Trotter number r needed.

B. Quantum Signal Processing

While most applications to date simulating relativistic quantum field theories use PFs as discussed in Sec. II A, there is an alternate approach for simulating the time evolution of quantum systems that is based on a very general technique called *Quantum Signal Processing* (QSP). There are two main motivations for studying QSP-based quantum simulation algorithms are: First they have a better asymptotic complexity than PFs [43, 44]. Second they are compatible with a wider class of Hamiltonians than those which can be efficiently mapped onto Pauli Hamiltonians, and for which the number of qubits is sublinear in the number of degrees of freedom in the system [33, 34, 47].

As with PFs, the aim of this section is a pedagogical overview of techniques based on QSP, however we do provide precise statements of the theorems needed in the rest of the paper. We will rely on results from the literature to provide proofs of these theorems.

Simulating the time evolution operator of a given Hamiltonian using QSP relies on a a few key insights, which we will now review in turn.

1. *Idea of block encoding*

Block encoding (BE) is a technique that allows one to implement the action of a given operator A on an arbitrary quantum state directly in a quantum circuit, despite this operator not being unitary. This can be accomplished by rescaling A and padding it with extra entries to fit it into a unitary matrix that can act simultaneously on the given quantum state together with an appropriate number of ancilla qubits. Schematically, this means that the operator A, which acts on a system Hilbert space $\mathcal{H}_s$, is embedded into a unitary matrix acting on a larger Hilbert space $\mathcal{H}_a \otimes \mathcal{H}_s$, where $\mathcal{H}_a$ is the Hilbert space of the ancillary qubits. Schematically, U_A is given by

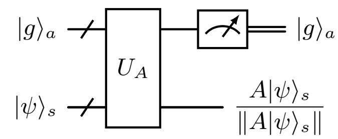

Figure 1. Circuit implementing the block encoding U_A of an operator A, as defined in Eq. (23). If the ancillary register is measured in the state $|g\rangle_a$, the state of the system is $A|\psi\rangle_s/\|A|\psi\rangle_s\|$.

$$U_A = \begin{pmatrix} A/\alpha & * \\ * & * \end{pmatrix}. \tag{23}$$

The rescaling by the parameter α, known as *scale factor*, is required, since the norm of any subblock of a unitary matrix has to be less than unity. Eq. (23) therefore implies that U_A is, in fact, a BE for the entire equivalence class of matrices A differing by a constant factor.

If we define the state $|g\rangle_a$ as the state that projects out the block of U_A containing the operator A/α, we can write

$$\begin{aligned} A/\alpha &= (\langle g|_a \otimes \mathbb{1}_s) U_A (|g\rangle_a \otimes \mathbb{1}_s) \qquad (24)\\ |g\rangle_a |\psi\rangle_s &= \begin{pmatrix} |\psi\rangle_s \\ 0 \end{pmatrix}_a \\ U_A |g\rangle_a |\psi\rangle_s &= \begin{pmatrix} A|\psi\rangle_s \\ * \end{pmatrix} = |g\rangle_a (A|\psi\rangle_s) + |\perp\rangle_{as}, \end{aligned}$$

where $|\perp\rangle_{as}$ is a vector perpendicular to $|g\rangle_a$. This implies that A is only applied to $|\psi\rangle_s$ iff the ancillary register is measured in $|g\rangle_a$. We shall term the probability of this to happen "success probability of the block encoding".

The success probability depends on how exactly U_A is constructed. In order for the algorithm to be considered efficient, the success probability has to scale inverse polynomially with problem parameters. The scale factor plays its role in defining the complexity of the simulation algorithm, as will be discussed later.

In much of this work we will use this technique to block encode a Hamiltonian H, and we call the corresponding BE U_H. The scale factor can then be absorbed by evolving a rescaled Hamiltonian

$$\tilde{H} = H/\alpha, \tag{25}$$

for the time

$$\tilde{t} = \alpha\, t\,, \tag{26}$$

so that

$$Ht = \tilde{H}\tilde{t}\,. \tag{27}$$

In the following discussion, we will choose a diagonal basis for the (rescaled) system Hamiltonian, such that basis vectors of the system Hilbert space are eigenstates of the Hamiltonian

$$\tilde{H}|\lambda\rangle_s = \lambda|\lambda\rangle_s\,, \tag{28}$$

with $|\lambda| < 1$. This basis is used only to simplify the discussion of the technique. Being able to diagonalize the Hamiltonian is not required for its use.

As already discussed, the vector $|g\rangle_a$ of the ancillary Hilbert space $\mathcal{H}_a$ defines the block in which the Hamiltonian is encoded in the unitary matrix U_H. In other words, the BE acts on the tensor product of a state $|\lambda\rangle_s$ and $|g\rangle_a$ as

$$U_H|g\rangle_a|\lambda\rangle_s = \lambda\,|g\rangle_a|\lambda\rangle_s + \sqrt{1-\lambda^2}|\perp^\lambda\rangle_{as}\,, \tag{29}$$

where we have defined a normalized transverse state that is orthogonal to the vector $|g\rangle_a$, such that $(\langle g|_a \otimes \mathbb{1}_s)|\perp\rangle_{as} = 0$. Thus, the action of $\tilde{H}$ can be extracted by acting with U_H on an enlarged Hilbert space and post-selecting on the ancilla qubit being in the $|g\rangle_a$ state, *i.e.*

$$\langle g|_a U_H|g\rangle_a|\lambda\rangle_s = \lambda\,|\lambda\rangle_s\,. \tag{30}$$

Note that if the ancillary Hilbert space $\mathcal{H}_a$ is 2-dimensional, one could choose $|g\rangle_a = |0\rangle_a$ and $|\perp\rangle_a = |1\rangle_a$.

Many different techniques for BE have been discussed in the literature. Among many others, one can use general algorithms such as the FABLE algorithm [48], approaches that rely on a technique called linear combination of unitaries (LCU) [29, 49], a technique called QETU [30], and techniques using access to the matrix elements of the sparse matrix and compact mappings H [31, 33, 34, 44, 49, 50]. The choice of BE is typically dictated by the number of ancillary qubits required, the value of the scale factor α, the gate complexity required for its implementation, whether an approximate implementation of the Hamiltonian is sufficient, and whether it is applicable to general sparse Hamiltonians.

One issue with BEs discussed so far is that the action of the BE does not stay in the Hilbert space spanned by $\mathrm{span}\{|g\rangle_a|\lambda\rangle_s, |\perp^\lambda\rangle_{as}\}$. In other words, the action of U_H on $|\perp^\lambda\rangle_{as}$ can produce a state with different value of $\lambda' \neq \lambda$, such that in general

$$\begin{aligned}\langle g|_a\langle\lambda'|_s U_H|g\rangle_a|\perp^\lambda\rangle_{as} &\neq 0\\ \langle\perp^{\lambda'}|_{as}U_H|\perp^\lambda\rangle_{as} &\neq 0\,.\end{aligned} \tag{31}$$

Therefore, repeated actions of the unitary U_H are not easily known. This can be dealt with by constructing a more constrained BE W_H, for which one can ensure that multiple actions of this BE on a given eigenstate will never produce a state with a different eigenvalue. This constrained BE is called a *qubitized block encoding* and is discussed in the following section.

2. LCU and other techniques for block encoding

We begin this section by reviewing a generic subroutine, Linear Combination of Unitaries (LCU) which, *inter alia*, can be used as a general-purpose technique for constructing BEs of qubit Hamiltonians. Then we briefly discuss several modifications of LCU as well as alternative approaches to constructing BEs.

Consider the situation were one has a combination of M unitary operators $U_0, \ldots, U_{M-1}$, each acting on a system Hilbert space $\mathcal{H}_s$ and the goal is to construct the operator

$$T = \sum_{i=0}^{M-1} \beta_i\, U_i\,, \tag{32}$$

acting on the same system Hilbert space.[7] [8]

This can be achieved in the following way. First, consider an ancilla register with Hilbert space $\mathcal{H}_a$ containing $k = \lceil \log M \rceil$ qubits. Labeling the computational basis of these states through the integers corresponding to the binary string encoded in the qubits, one defines a so-called PREPARE oracle to create a state $|\beta\rangle$:

$$|\beta\rangle_a = \text{PREPARE}_a|0\rangle_a = \frac{1}{\sqrt{\beta}}\sum_{i=0}^{M-1}\sqrt{\beta_i}|i\rangle_a\,, \tag{33}$$

where $|0\rangle_a$ corresponds to the state with all qubits in $\mathcal{H}_a$ in the $|0\rangle_a$ state and we have defined $\beta \equiv \|\vec{\beta}\|_1 = \sum_i |\beta_i|$.

Next, using the so-called SELECT oracle, one performs operations U_i on states in $\mathcal{H}_s$, controlled on the values of qubits in $\mathcal{H}_a$

$$\text{SELECT} = \sum_{i=0}^{M-1} |i\rangle_a\langle i|_a \otimes U_i\,. \tag{34}$$

---

[7] We assume $\beta_i > 0$ since the complex phases of β_i can be absorbed by U_i.

[8] This technique can also be used to add non-unitary operators by first block-encoding them and then adding the unitaries using LCU.

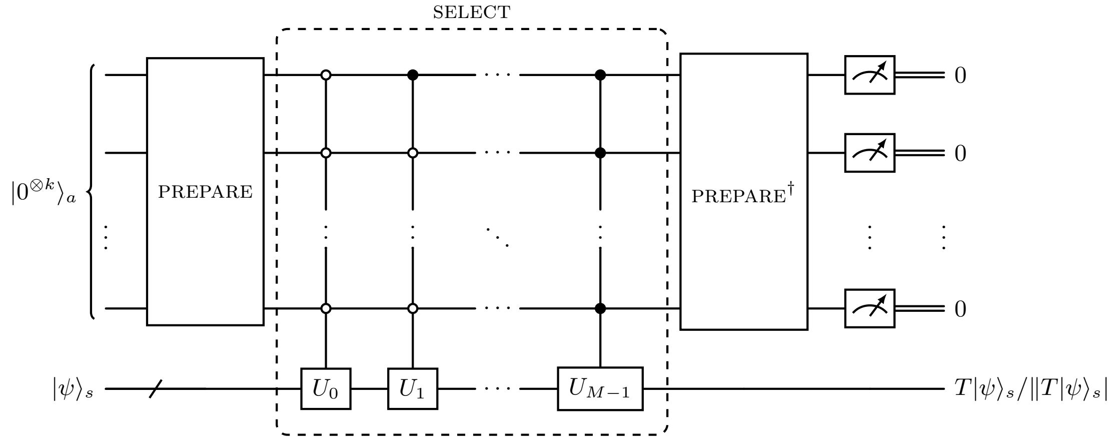

Figure 2. Linear Combination of Unitaries (LCU) implements the BE U_T of an operator T expressed as a sum of elementary operators with known circuit implementations, reproduced from Ref. [29]. Each operator U_i is controlled on the binary string representing its index i. The size of the ancillary register is $k = \lceil \log_2 M \rceil$. For illustration purposes, $\log_2(M)$ is assumed to be an integer k such that the binary string of $M-1$ contains all 1's.

At the end one reverses the prepare oracle. The complete circuit on the Hilbert space $\mathcal{H}_{as} = \mathcal{H}_a \otimes \mathcal{H}_s$ can therefore be written as

$$U_T = \left(\text{PREPARE}_a^\dagger \otimes \mathbb{1}_s\right) \text{SELECT} \left(\text{PREPARE}_a \otimes \mathbb{1}_s\right). \tag{35}$$

Letting this operator act on a state $|0\rangle_a |\psi\rangle_s$ one finds

$$U_T |0\rangle_a |\psi\rangle_s = \frac{1}{\beta} |0\rangle_a T |\psi\rangle_s + |\perp\rangle_{as}, \tag{36}$$

where $|\perp\rangle$ is an unnormalized state transverse to $(|0\rangle_a \otimes \mathbb{1}_s)$. This implies that U_T is a BE of T.

From the above discussion it is clear that the number of ancilla qubits to combine M unitaries is given by $\dim(\mathcal{H}_a) \sim \log M$, and the number of gates is given by M gates that are controlled on $\log M$ qubits, which can be reduced to $\mathcal{O}(M \log M)$ elementary gates.

While the presented approach to LCU relies on the binary encoding of terms on the RHS of Eq. (32) in the ancillary register, other encodings can be used as well. In particular, a variation of the LCU algorithm exists, which takes advantage of the Hamiltonian locality [51]. For an k-local $\mathsf{n_q}$-qubit Hamiltonian, it requires $2\mathsf{n_q}$ ancillary qubits yet only uses $2k$-controlled gates.

The LCU algorithm can be applied to a Hamiltonian provided in a form of a $2^{\mathsf{n_q}} \times 2^{\mathsf{n_q}}$ matrix, upon decomposing it into Pauli strings as $H = \sum_{i=0}^{4^{\mathsf{n_q}}-1} \beta_i P_i$, where P_i are the Pauli strings and the coefficients c_i are found as $c_i = \frac{1}{2^{\mathsf{n_q}}} \operatorname{Tr}(H P_i)$. An alternative approach to constructing BEs for Hamiltonians given in the matrix form is considered in Ref. [48].

The LCU approach is often combined with other methods. In Secs. IV C 2 and IV C 3 we shall consider its modifications which take into account the structure of particular lattice Hamiltonians.

Lastly, we briefly mention that simulation techniques based on BE, considered in the next section, are compatible with a wide class of *sparse* Hamiltonians, including those which cannot be efficiently mapped onto Pauli strings. A general approach to constructing BEs for such systems is based on the usage of *sparse oracle* subroutines. As was mentioned in Sec. I, their construction is highly problem-specific [31–35] and does not seem to provide advantage over LCU for local HLFTs [35], which are considered the main application of this work.

3. *Qubitization*

A *qubitized block encoding* W_H of the Hamiltonian is a BE which remains in the subspace of $\operatorname{span}\{|g\rangle_a |\lambda\rangle_s, |\perp^\lambda\rangle_{as}\}$ such that one has

$$\begin{aligned} W_H |g\rangle_a |\lambda\rangle_s &= \lambda\, |g\rangle_a |\lambda\rangle_s - \sqrt{1-\lambda^2} |\perp^\lambda\rangle_{as} \\ &= \left(\lambda\, |g\rangle_a - \sqrt{1-\lambda^2} |\perp^\lambda\rangle_a\right) |\lambda\rangle_s, \end{aligned} \tag{37}$$

where we have defined $|\perp^\lambda\rangle_{as} \equiv |\perp^\lambda\rangle_a |\lambda\rangle_s$ for all eigenstates $|\lambda\rangle$. Note that the minus sign between the two terms is conventional. The orthogonal state $|\perp^\lambda\rangle_a$ can now be defined as

$$|\perp^\lambda\rangle_a |\lambda\rangle_s = \frac{\lambda \mathbb{1}_{as} - W_H}{\sqrt{1-\lambda^2}} |g\rangle_a |\lambda\rangle_s. \tag{38}$$

This works for any dimension of the ancilla Hilbert space $\mathcal{H}_a$, and implies that for each eigenvalue λ of the Hamiltonian there is one specific transverse vector in $\mathcal{H}_a$.

Eq. (37) implies the operator W_H is block diagonal, and is given by

$$\left(\mathbb{1}_a \otimes \langle\lambda'|_s\right) W_H \left(\mathbb{1}_a \otimes |\lambda\rangle_s\right) = W_H^{(\lambda)} \delta_{\lambda\lambda'} , \tag{39}$$

with $W_H^{(\lambda)}$ acting on the two-dimensional Hilbert space $\text{span}\{|g\rangle_a, |\perp^\lambda\rangle_a\} \in \mathcal{H}_a$

$$\begin{aligned} W_H^{(\lambda)} &= \begin{pmatrix} \lambda & -\sqrt{1-\lambda^2} \\ \sqrt{1-\lambda^2} & \lambda \end{pmatrix}_a \\ &= \exp(-iY_a\theta_\lambda) , \end{aligned} \tag{40}$$

where Y_a is the Pauli-y operator acting on the qubit $|a\rangle$ and

$$\theta_\lambda = \cos^{-1}(\lambda) . \tag{41}$$

While so far we have only defined the unitary W_H through its action on a given state, a very important result is that it can be obtained from a general (not qubitized) BE U_H. The basic idea is to construct orthogonal subspaces using a Gram-Schmidt procedure, and then implementing this through appropriate basis rotations. This construction requires adding one qubit $|q\rangle$ to the ancillary Hilbert space, such that $\mathcal{H}_a \to \mathcal{H}_{qa} = \mathcal{H}_q \otimes \mathcal{H}_a$. In this new ancillary Hilbert space we define

$$|g\rangle_{qa} = |+\rangle_q |g\rangle_a , \tag{42}$$

and the operator W_H is defined on the Hilbert space $\mathcal{H}_{qas} = \mathcal{H}_q \otimes \mathcal{H}_a \otimes \mathcal{H}_s$. As was shown in Section 4

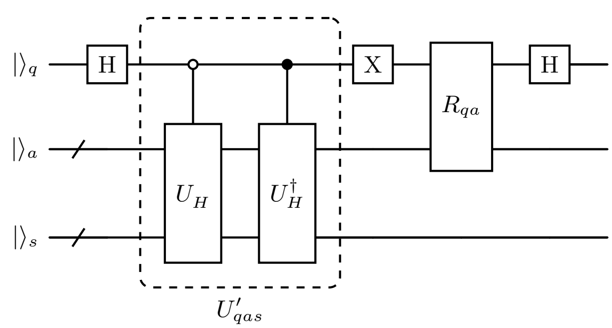

Figure 3. Circuit for the qubitized block encoding W_H, given an arbitrary block encoding U_H. The circuit for R_{qa} is shown in Fig. 4.

of [44], it is given by

$$\begin{aligned} W_H =& (\mathrm{H}_q \otimes \mathbb{1}_{as})(R_{qa} \otimes \mathbb{1}_s)(\mathrm{X}_q \otimes \mathbb{1}_{as}) \\ & \times U'_{qas}(\mathrm{H}_q \otimes \mathbb{1}_{as}) , \end{aligned} \tag{43}$$

where H_q and X_a are the Hadamard and X gate on the qubit $|q\rangle$, R_{qa} is a standard reflection operator

$$R_{qa} = 2|g\rangle_a|+\rangle_q\langle+|_q\langle g|_a - \mathbb{1}_{qa} , \tag{44}$$

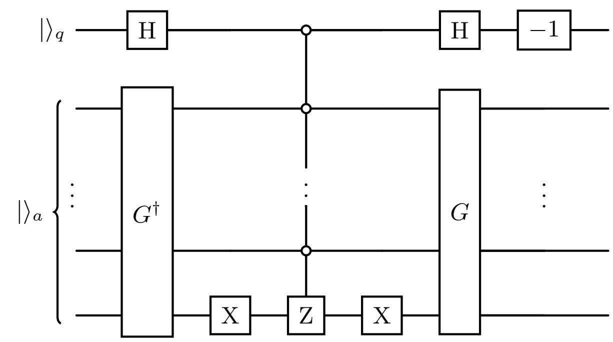

Figure 4. Circuit for the reflection operator R_{qa} defined in Eq. (44) and used in Eq. (43), see Ref [49] for alternative implementations. G is the oracle for preparing the state $|g\rangle_a$, i.e. $G|0\rangle_a = |g\rangle_a$. The $\boxed{-1}$ gate adds an overall phase to the circuit (negative sign), and can be implemented, e.g., as XZXZ.

and

$$U'_{qas} = |0\rangle_q\langle 0|_q U_H + |1\rangle_q\langle 1|_q U_H^\dagger , \tag{45}$$

is an operator that applies the U_H or $U_H^\dagger$ operator, depending on the state of $|q\rangle$.

One can show through explicit computation that

$$W_H|g\rangle_{qa}|\lambda\rangle_s = \left(\lambda\,|g\rangle_{qa} - \sqrt{1-\lambda^2}|\perp^\lambda\rangle_{qa}\right)|\lambda\rangle_s , \tag{46}$$

with

$$|\perp^\lambda\rangle_{qa} = |-\rangle_q|\perp^\lambda\rangle_a , \tag{47}$$

verifying that Eq. (37) gives indeed a qubitized BE of H. The circuits for operators W_H, U'_{qas}, and R_{qa} are shown in Figs. 3 and 4.

This qubitized BE gives the same result as the original BE U_H when acted on $|g\rangle_{qa}|\lambda\rangle_s$, but it has a much simpler structure when applied multiple times. Since W_H is block diagonal, one finds

$$\left(\mathbb{1}_{qa} \otimes \langle\lambda'|_s\right)(W_H)^k \left(\mathbb{1}_{qa} \otimes |\lambda\rangle_s\right) = \left(W_H^{(\lambda)}\right)^k \delta_{\lambda'\lambda} , \tag{48}$$

and one can show that

$$\begin{aligned} \left(W_H^{(\lambda)}\right)^k &= \begin{pmatrix} T_k(\lambda) & -\sqrt{1-\lambda^2}\,U_{k-1}(\lambda) \\ \sqrt{1-\lambda^2}\,U_{k-1}(\lambda) & T_k(\lambda) \end{pmatrix}_{qa} \\ &= \exp\left(-i(Y_{qa} \otimes \mathbb{1}_s)k\theta_\lambda\right) . \end{aligned} \tag{49}$$

Here $T_k(\lambda)$ and $U_k(\lambda)$ are Chebyshev polynomials of the first and second kind, respectively. Given that Chebyshev polynomials are an excellent polynomial basis for approximating L^∞ functions on an finite interval, one can hope to construct a general function of the eigenvalues (and therefore of the Hamiltonian matrix itself) by combining powers of the W_H operator. In the next section we discuss how the time evolution operator can be approximated using this technique.

4. Calculating the time evolution operator using QSP

In order to use the operator W_H of the previous section to calculate the exponential of the Hamiltonian, we first note that the qubitized operator W_H can be diagonalized by defining the states

$$|\theta_\pm^\lambda\rangle_{qas} \equiv \frac{1}{\sqrt{2}}\left(|g\rangle_{qa} \pm i|\perp^\lambda\rangle_{qa}\right)|\lambda\rangle_s\,. \tag{50}$$

Using Eq. (37) one can easily show that

$$W_H|\theta_\pm^\lambda\rangle_{qas} = \mathrm{e}^{i\theta_\pm^\lambda}|\theta_\pm^\lambda\rangle_{qas}\,, \tag{51}$$

with

$$\theta_\pm^\lambda = \mp\cos^{-1}(\lambda)\,. \tag{52}$$

Given this form, one can now define a new operator $V_H(\phi)$, which depends on the value of an angle ϕ and which can be constructed from the operator W_H. It requires one more ancillary qubit $|b\rangle \in \mathcal{H}_b$, such that the operator $V_H(\phi)$ acts on the Hilbert space $\mathcal{H}_{bqas} \equiv \mathcal{H}_b \otimes \mathcal{H}_q \otimes \mathcal{H}_a \otimes \mathcal{H}_s$. It is defined by (see Fig. 6)

$$V_H(\phi) = (\mathrm{e}^{-i\phi Z_b/2} \otimes \mathbb{1}_{qas})W'(\mathrm{e}^{i\phi Z_b/2} \otimes \mathbb{1}_{qas})\,, \tag{53}$$

where Z_b is the usual Pauli Z operator acting on the qubit $|b\rangle$, and $\tilde{W}$ is the W_H operator controlled on the $|b\rangle$, which now acts on the Hilbert space $\mathcal{H}_{bqas}$:

$$W' = \mathbb{1}_{qas}|+\rangle_b\langle+|_b + W_H|-\rangle_b\langle-|_b\,. \tag{54}$$

One can show through explicit computation that

$$\begin{aligned}\left(\mathbb{1}_b \otimes \langle\theta_\pm^{\lambda'}|_{qas}\right) V_H(\phi)\left(\mathbb{1}_b \otimes |\theta_\pm^\lambda\rangle_{qas}\right)& \\ = V_H^{(\theta_\pm^\lambda)}(\phi)\,\delta_{\lambda\lambda'}\,,&\end{aligned} \tag{55}$$

with

$$\begin{aligned}V_H^{(\theta)}(\phi) &= \mathrm{e}^{i\frac{\theta}{2}}\begin{pmatrix}\cos\frac{\theta}{2} & -i\sin\frac{\theta}{2}\mathrm{e}^{-i\phi}\\ -i\sin\frac{\theta}{2}\mathrm{e}^{i\phi} & \cos\frac{\theta}{2}\end{pmatrix}_b \\ &= \mathrm{e}^{i\frac{\theta}{2}}\mathrm{e}^{-i\frac{\theta}{2}(X_b\cos\phi + Y_b\sin\phi)}\,,\end{aligned} \tag{56}$$

where X_b and Y_b denote the Pauli-x and y matrices in $\mathcal{H}_b$.

What this construction has accomplished is to create a unitary operator $V_H(\phi)$ that is block diagonal in the original Hilbert space $\mathcal{H}_s$, with the entries of the 2×2 matrix in $\mathcal{H}_b$ given by functions of the eigenvalues of the Hamiltonian (through $\cos\theta_\pm^\lambda$), parameterized by some ϕ. By multiplying several of these operators in sequence (each with a different value of ϕ),

$$V_H^{(\theta)}(\vec{\phi}) \equiv V_H^{(\theta)}(\phi_{N_\phi})\ldots V_H^{(\theta)}(\phi_1)\,, \tag{57}$$

one obtains an operator that is still block diagonal in $\mathcal{H}_s$. $V_H^{(\theta)}(\vec{\phi})$ is a 2×2 matrix in $\mathcal{H}_b$, which can be expressed using the Pauli decomposition

$$V_H^{(\theta)}(\vec{\phi}) = A(\theta)\mathbb{1}_b + iB(\theta)X_b + iC(\theta)Y_b + iD(\theta)Z_b\,. \tag{58}$$

The functions $A(\theta)\ldots D(\theta)$ are all parameterized by the angles $\vec{\phi} = (\phi_1,\ldots,\phi_{N_\phi})$. The type of functions that can be obtained for different choices of $\vec{(\phi)}$ were studied in [53] and it was shown that one can choose values of $\vec{\phi}$ to obtain functions A and C of the form

$$\begin{aligned}|A^2(\theta)| + |C^2(\theta)| \leq 1\,,&\qquad A(0) = 1\\ A(\theta) = \sum_{k=0}^{N_\phi/2} a_k\cos(k\theta)&\\ C(\theta) = \sum_{k=1}^{N_\phi/2} c_k\sin(k\theta)\,.&\end{aligned} \tag{59}$$

Reversing this logic, one can start from some desired functions $A(\theta)$, $C(\theta)$, and determine phases $\vec{(\phi)}$ such that $V_H^{(\theta)}(\vec{\phi})$ reproduces these functions (approximately). This can be accomplished using an efficient classical procedure given in Ref. [53].[9]

We omit now a few final details, all of which are straightforward and can be found in Ref. [44], and simply state the relevant results. As can be confirmed from Eq. (58), letting the operator $V_H^{(\theta)}(\vec{\phi})$ act on the state $|+\rangle_b$ and post-selecting on $\langle+|_b$ picks out the function

$$\begin{aligned}\langle+|_b\langle g|_{qa}\langle\lambda'|_s V_H(\vec{\phi})|+\rangle_b|g\rangle_{qa}|\lambda\rangle_s&\\ = \delta_{\lambda\lambda'}\left[\tilde{A}(\lambda) + i\tilde{C}(\lambda)\right].&\end{aligned} \tag{60}$$

The functions $\tilde{A}(\lambda)$ and $\tilde{C}(\lambda)$ are directly related to the functions $A(\theta_\lambda)$, $C(\theta_\lambda)$, with the detailed relation given in Ref. [44]. The success probability for

[9] A recent version of QSP promises a lower cost of calculating phases $\vec{\phi}$ [54].

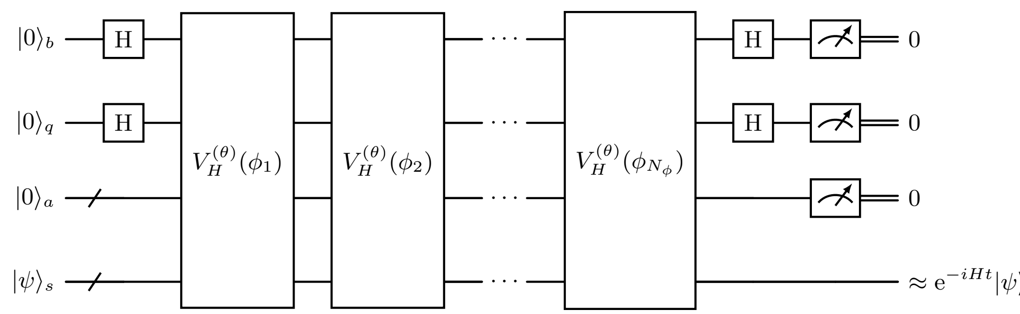

Figure 5. Quantum Signal Processing (QSP) circuit used for simulating time evolution, reproduced from Ref. [52]. The circuit prepares a block encoding for the approximation of the time evolution operator $\mathrm{e}^{-iHt}|\psi\rangle$. Circuit for $V_H^{(\theta)}(\phi)$ is shown in Fig. 6. When all the ancillary qubits are measured in the zero states, the desired operator is applied to the system register $|\psi\rangle_s$. Without loss of generality, $|g\rangle_a$ is set to $|g\rangle_a = |0\rangle_a$.

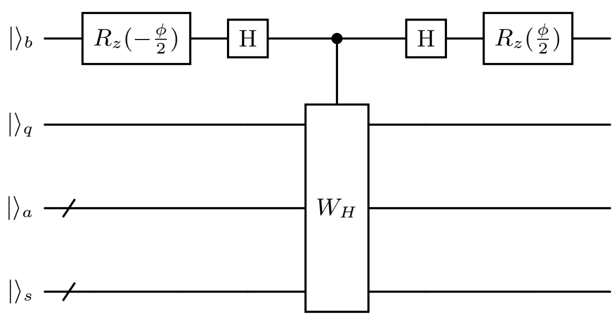

Figure 6. Circuit for $V_H^{(\theta)}(\phi)$, as defined is Eq. (56).

measuring the system in the state $|+\rangle_b|g\rangle_{qa}$ for a given value λ depends on the functions and is given by

$$p \geq |\tilde{A}^2(\lambda)| + |\tilde{C}^2(\lambda)|\,. \tag{61}$$

An efficient classical algorithm exists that finds phases $\vec{\phi}$ such that one can approximate the time evolution operator with uncertainty bounded by ε

$$\left|\mathrm{e}^{i\lambda\tilde{t}} - [\tilde{A}(\lambda) + i\tilde{C}(\lambda)]\right| < \varepsilon\,. \tag{62}$$

This is related to the fact that products of qubitized BEs give rise to Chebyshev polynomials, which can be used to approximate the real and imaginary part of $\mathrm{e}^{i\lambda t}$ through the Jacobi-Anger expansion. In this case, the circuit in Fig. 5 would implement the approximate BE of the evolution operator e^{-iHt}. The number of phases needed for a given value of ε is bounded by

$$N_\phi = \mathcal{O}\Big(\tilde{t} + \log(1/\varepsilon)\Big) = \mathcal{O}\big(\alpha t + \log(1/\varepsilon)\big)\,. \tag{63}$$

Note also that Eqs. (61) and (62) imply that

$$p \geq 1 - \mathcal{O}(\varepsilon)\,, \tag{64}$$

since the time evolution operator has unit magnitude.

It is worth mentioning that the success rate of QSP is always $\mathcal{O}(1)$, independent of the success rate of the BE used. This is due to the fact that we have used QSP to implement a unitary function (e^{-iHt}) which has unit norm. This implies that $\tilde{A}(\lambda)^2 + \tilde{C}(\lambda)^2 \approx 1$, which together with Eq. (61) gives a success probability that is close to one.

Before we conclude, we should mention that we have focused here on using QSP to simulate the time evolution operator, which required a particular form of the polynomial functions. QSP is more general than that, and other functions can be implemented as well, some of which require less resources than the case discussed here. For more details, we find [49] a useful reference.

C. HHKL

The results presented so far (PFs and QSP) can be applied to general site-local Hamiltonians (see Definition 2). For geometrically-site-local Hamiltonians (see Definition 3) one can use the fact that information from one area of the lattice can only spread to areas not directly connected to it through repeated actions of the time evolution operators, which implies that the speed with which this information spreads is bounded. This is formalized by the Lieb-Robinson bound [55]. This idea was used in a paper by Haah, Hastings, Kothari and Low (HHKL) [45] to devise a scheme for simulating the time evolution of geometrically-site-local Hamiltonians.

As before, this section is aimed at giving the reader a basic understanding of the technique, without going into too many of the details. In order to understand these details the reader is encouraged to read the excellent description of the algorithm in the original work, where all statements are also carefully proved.

The main ingredient to the HHKL algorithm is that the time evolution of a large quantum system with geometrically local Hamiltonian can be obtained from the time evolution of two smaller systems that share some overlap, which has to be of at least the size given by the ball of size $\mathcal{O}(1)$ used in Definition 3. Thus, the system Hilbert space $\mathcal{H}_s$ is divided into three parts, $\mathcal{H}_{a,b,c}$ such that $\mathcal{H}_s = \mathcal{H}_a \otimes \mathcal{H}_b \otimes \mathcal{H}_c$. In the discussion of Ref. [45] is assumed that the local Hamiltonian H_J such that $||H_J|| \leq 1$. Thus, in the remainder we work with

$$\tilde{H}_J = \frac{H_J}{||H_J||}\,, \qquad \tilde{t} = ||H_J||t\,. \tag{65}$$

First, one uses that the evolution of a system for some long time $\tilde{t}$ can be split into the product of unitaries over shorter times $\Delta t = \mathcal{O}(1)$:

$$U(\tilde{t},0) = U(\tilde{t},\tilde{t}-\Delta t)\cdots U(\Delta t,0)\,. \tag{66}$$

The total number of such unitaries is $\mathcal{O}(\tilde{t})$.

Lemma 6 of Ref. [45] states that the time evolution $U_s(\Delta t)$ of a Hamiltonian on the whole system over time Δt can be obtained by multiplying together the forward time evolution in the system $\mathcal{H}_{b\cup c} = \mathcal{H}_b \otimes \mathcal{H}_c$ and $\mathcal{H}_{b\cup c} = \mathcal{H}_b \otimes \mathcal{H}_c$ and the backwards evolution in the system $\mathcal{H}_b$ as

$$U_{a\cup b\cup c}(\Delta t) = U_{a\cup b}(\Delta t) U_b^\dagger(\Delta t) U_{b\cup c}(\Delta t) + \mathcal{O}(\delta)\,, \tag{67}$$

where the error in the approximation is given by

$$\delta \equiv \delta(a,b,c) = \mathrm{e}^{-\mu\,\mathrm{d}(a,c)} \sum_{X\in \mathrm{BD}(ab,c)} ||\tilde{H}_X||\,. \tag{68}$$

For now we assume that each of the $U(\Delta t)$ on the RHS of Eq. (67) is implemented exactly. In Eq. (68) μ is some constant, $\mathrm{d}(a,c)$ is the smallest distance between any point in a and c, and the norm $||\tilde{H}_J||$ is summed over all terms that are on the boundary of $a\cup b$ and c, indicated by $\mathrm{BD}(ab,c)$. The total number of terms in this sum is $\mathcal{O}(\ell^{\mathsf{d}-1})$. The uncertainty is therefore exponentially suppressed in the distance between the regions a and c. This implies that this approximation works well for large enough distance $\ell \equiv \mathrm{d}(a,c)$.

This result can be applied recursively, splitting the evolution into smaller and smaller pieces, which just have to be larger than the size of the ball $\mathcal{O}(1)$. If the size of the original system is given by L^{d} and the final pieces contain order ℓ^{d} lattice sites, one ends up with

$$m = \mathcal{O}\left(\frac{L^{\mathsf{d}}}{\ell^{\mathsf{d}}}\right) \tag{69}$$

individual pieces. Taking into account the $\tilde{t}$ evolution operators we started from, the final error in the evolution is given by $\tilde{t}\,m, \delta$. In order to have the final error of order the exponentiation error ε therefore requires

$$\delta = \mathcal{O}\left(\frac{\varepsilon}{\tilde{t}\,m}\right). \tag{70}$$

Equating Eqs. (68) and (70) one finds that this can be satisfied if one uses

$$\ell = \Theta\left(\log\left(\frac{L^{\mathsf{d}}\tilde{t}}{\varepsilon}\right)\right). \tag{71}$$

One can then estimate the required resources using the fact that one needs to compute

$$\mathcal{O}(Tm) = \mathcal{O}\left(L^{\mathsf{d}}\tilde{t}\log^{-\mathsf{d}}\left(\frac{L^{\mathsf{d}}\tilde{t}}{\varepsilon}\right)\right) \tag{72}$$

time evolution operators on a system of size $\mathcal{O}(\ell^{\mathsf{d}})$.[10] The cost and the associated additional error for implementing each of these "local" pieces depends on the algorithm used for their implementation.

D. QETU

In this section, we review the Quantum Eigenvalue Transformation for Unitary Matrices (QETU) developed in Ref. [30]. We then describe a novel application of QETU to implement BEs based off a method in Ref. [42]. In this section we only discuss the details relevant to our implementation, and further details can be found in the original references.

The Quantum Eigenvalue Transformation for Unitary Matrices (QETU) is very similar to the QSP method described in Sec. II E 2 in that it allows one to implement general matrix functions of some Hermitian operator A by performing repeated calls to some fundamental building block. The major difference of QETU is that, instead of performing repeated calls to a BE U_A as with QSP, the building block for QETU is the time-evolution operator $\mathrm{e}^{-i\tau A}$ for some small time τ. The "U" in QETU indicates that the building block in the circuit is a unitary matrix. In a broad sense, QETU replaces the BE U_A in the QSP circuit in Fig. 5 with the controlled time-evolution

[10] Note that decreasing ε is logarithmically decreasing the number of evolution operators. This number clearly has to be larger than unity, meaning ε cannot be exponentially small with system size.

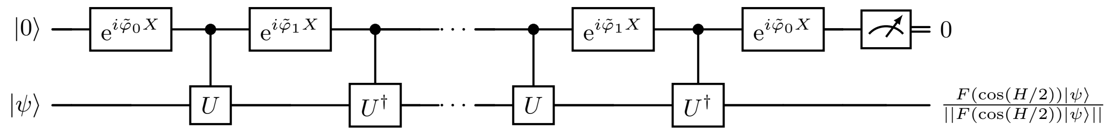

Figure 7. Circuit diagram for QETU. The top qubit is the control qubit and the bottom register is the state that the matrix function is applied to. Here $U = \mathrm{e}^{-i\tau A}$ is the time evolution circuit. If the control qubit is measured to in the zero state, one prepares the normalized quantum state $F(\cos(\tau A/2))|\psi\rangle/||F(\cos(\tau A/2))|\psi\rangle||$ for some even polynomial $F(x)$. For symmetric phase factors $(\tilde{\varphi}_0, \tilde{\varphi}_1, \ldots, \tilde{\varphi}_1, \tilde{\varphi}_0) \in \mathbb{R}^{d+1}$, the function $F(x)$ is a real even polynomial of degree d. The probability of measuring the control qubit in the zero state is $p = ||F(\cos(\tau A/2))|\psi\rangle||^2$.

operator $\mathrm{e}^{-i\tau A}$. One major difference is that QETU implements real functions with definite parity. Constructing functions without definite parity or complex functions can be achieved by using QETU to implement the components with definite parity, and then using LCU to add the pieces together.

The QETU circuit is shown in Fig. 7. One nice property of QETU is that it requires only a single ancillary qubit, the so-called control qubit. By repeatedly performing controlled calls to $U = \mathrm{e}^{-i\tau A}$ alternated with rotation gates and post-selecting the control qubit on the zero state, one implements the even matrix function $F(\cos(\tau A/2))$ on the state register[11], where the function F is parameterized by the angles $\vec{(\phi)}$, similar to the case in QSP. As was done there, we require $|F(x)| \leq 1 \forall x \in [-1, 1]$. The success probability of measuring the control qubit in the zero state is $||F(\cos(\tau A/2))|\psi\rangle||$[12]. In practice, the QETU circuit is used for approximately implementing $\mathsf{f}(A)$ by realizing a transformation $F(\cos(\tau A/2))$, where $F(x)$ is a polynomial approximation to $\mathsf{F}(x) \equiv \mathsf{f}(\frac{2}{\tau}\arccos(x))$. We now describe our proposal for implementing BEs using QETU.

Suppose we want to prepare some function $\mathsf{f}(A)$ of a diagonal Hermitian matrix A with known eigenvalues $A|a_j\rangle = a_j|a_j\rangle$. Furthermore, define $a_{\max} \equiv \max(a_j)$ and $a_{\min} \equiv \min(a_j)$. Because QETU returns a function of a periodic argument, *i.e.* $F(\cos(\tau A/2))$, any function constructed using QETU will repeat itself for large values of a_j. To avoid this complication, the original algorithm [30] proposed to shift the spectrum of A to the limited range $[\eta, \pi - \eta]$ for some $\eta > 0$. This was crucial to guarantee isolation of the ground state when using QETU for state preparation. Furthermore, it was shown in Ref. [42] that shifting the spectrum of the operator A to be in this limited range and allowing η to be a free parameter dramatically improved the convergence of the Chebyshev approximation to functions of the form $\mathsf{f}(A) \sim \mathrm{e}^{-A^2/\sigma^2}$. The shifted operator A_{sh} whose spectrum is in the range $[\eta, \pi-\eta]$ is given by

$$A_{\mathrm{sh}} = c_1 A + c_2 \,, \tag{73}$$

where

$$c_1 = \frac{\pi - 2\eta}{a_{\max} - a_{\min}} \,, \quad c_2 = \eta - c_1 a_{\min} \,. \tag{74}$$

Note that using $\mathrm{e}^{-i\tau A_{\mathrm{sh}}}$ as the building block in the QETU algorithm requires a modification to the function $\mathsf{F}(x)$. The desired function must satisfy $\mathsf{F}(\cos(\tau A_{\mathrm{sh}}/2) = \mathsf{f}(A)$, which implies

$$\mathsf{F}(x) = \mathsf{f}\left(\frac{\frac{2}{\tau}\arccos(x) - c_2}{c_1}\right) . \tag{75}$$

Now that we know the form of the function we wish to approximate, we make several observations.

First, even if the function $\mathsf{f}(x)$ has definite parity, the function $\mathsf{F}(x)$ will in general not have definite parity due to the presence of the $\arccos(x)$. This implies that one will have to implement the even and odd pieces of $\mathsf{F}(x)$ separately, and then add them using LCU. While there are no theoretical issues with this procedure for this application, it was found in Ref. [42] that using LCU introduced a large prefactor, and that the need to use LCU could be avoided altogether by choosing τ in such a way as to make $\mathsf{F}(x)$ have definite parity. To see this, note that if one chooses $\tau = \pi/c_2$, the function $\mathsf{F}(x)$ becomes

$$\mathsf{F}(x) = \mathsf{f}\left(-\frac{2}{\pi}\frac{c_2}{c_1}\arcsin(x)\right) , \tag{76}$$

where we have used $\arcsin(x) = \pi/2 - \arccos(x)$. Because $\arcsin(x)$ has odd parity, the function $\mathsf{F}(x)$ has the same parity as the function $\mathsf{f}(x)$, as desired.

---

[11] QETU relies on repeated calls to the controlled implementations of the time-evolution operator. While this does not change the asymptotic scaling, it introduces a large prefactor in the gate complexity. A control-free version of QETU was also presented in Ref. [30], which involves an operator dependent procedure. The procedure for diagonal Hermitian matrices can be found in Appendix B of Ref. [42].

[12] Note that the original algorithm set $\tau = 1$. It was shown in Ref. [42], however, that allowing τ to be a free parameter can reduce the cost of QETU for both ground-state preparation and implementation of Gaussian wavepackets.

Note that τ is a function of η through the parameter c_2, and one must choose a different τ for each η.

The second observation we make regarding $\mathsf{F}(x)$ is that, for general functions $\mathsf{f}(x)$, its first derivative diverges at $x = \pm 1$ due to the presence of the $\arcsin(x)$ (or $\arccos(x)$) term. Chebyshev approximations of functions with m continuous derivatives on $x \in [-1, 1]$ are known to converge polynomially to the true function with the typical rate $(1/n_{\mathrm{Ch}})^m$, where n_{Ch} is the number of Chebyshev polynomials used in the approximation [56]. If one needed to reproduce $\mathsf{F}(x)$ for all $x \in [-1, 1]$, this poor convergence would spoil the optimal scaling with precision. We now outline a method for overcoming this problem described in Ref. [42].

The key method we employ from Ref. [42] is to exploit the fact that the spectrum of the operator A_{sh} is known exactly (in our case, operators given in Eqs. (124) and (125) below play the role of A_{sh}), and therefore one only samples $\mathsf{F}(x)$ at those finitely many points. Because there are $\mathcal{O}(2^{\mathsf{n_q}})$ such values, one can reproduce the function at those points exactly by using $\mathcal{O}(2^{\mathsf{n_q}})$ Chebyshev polynomials. In this way, one avoids the poor polynomial convergence of the Chebyshev expansion at the cost of introducing an exponential scaling with $\mathsf{n_q}$. However, because digitization errors generally decrease exponentially with $\mathsf{n_q}$, one needs only small values of $\mathsf{n_q}$ and this exponential scaling will not be a computational bottleneck[13].

Once the Chebyshev polynomial has been determined, the next step is to calculate the phases φ appearing in the circuit in Fig. 7 The procedure to do this is given in Ref. [30], and an example code to calculate the phases has been implemented in QSPPACK [57]. Note that the classical cost of determining the phases was found to scale roughly quadratically with the number of phases. [42]. As described in Appendix B of Ref. [30], the phases in the QETU circuit $\{\tilde{\varphi}_j\}$ are related to the phases calculated using QSPPACK $\{\tilde{\phi}_j\}$ by $\tilde{\varphi}_j = \tilde{\phi}_j + (2 - \delta_{j\,0})\pi/4$

[13] Note that it was found in Ref. [42] that by increasing η, this polynomial convergence with the degree of the Chebyshev polynomial can be converted to exponential for the class of functions of the form $\mathsf{f}(x) = \mathrm{e}^{-x^2/\sigma^2}$. One issue with applying this method to our problem of $\mathsf{f}(x) = x^n$ is that, as η increases, the scale factor α diverges as $\eta \to \pi/2$, as can be seen in Eq. (149). For this reason, we fix $\eta = 0$ and produce the function exactly, and leave further optimizations for future work.

E. Summary and precise statement of techniques used

1. General product formulas

Definition 5. A p^{th} order PF $S_p(t)$ is a PF of the form (15), such that it approximates the true exponential e^{-iHt} to p^{th} order in t, i.e.,

$$\mathrm{e}^{-iHt} = S_p(t) + \mathcal{O}(t^{p+1})\,. \tag{77}$$

Theorem 6 (Trotter number with commutator scaling)**.** *Let $H = \sum_{\gamma=1}^{\Gamma} H_\gamma$ be an operator comprised of Γ Hermitian summands. Let $S_p(t)$ be a p^{th} order PF as defined by* (77)*, with $t \geq 0$. Then, if we require an exponentiation error $\mathcal{O}(\varepsilon)$, as defined by* (21)*, it suffices to choose*

$$r = \mathcal{O}\left(\frac{\tilde{\alpha}^{\frac{1}{p}} t^{1+\frac{1}{p}}}{\varepsilon^{\frac{1}{p}}}\right), \tag{78}$$

where $\tilde{\alpha} \equiv \sum_{\gamma_1,\gamma_2,\ldots,\gamma_{p+1}=1}^{\Gamma} |||[H_{\gamma_{p+1}}, \ldots [H_{\gamma_2}, H_{\gamma_1}]]|||$

Proof. This theorem follows directly from Theorem 11 and Corollary 12 of [28]. □

2. Quantum Signal Processing

In this section we summarize the results of the section on QSP in a concise and precise form which will be referred to later in the text.

Definition 7 (Block encoding)**.** Let H be a Hamiltonian acting on the n-qubit Hilbert space $\mathcal{H}_s \cong \mathbb{C}^{2^n}$. Let $k \geq 0$ be an integer and let U_H be a unitary operator on the joint Hilbert space $\mathcal{H}_a \otimes \mathcal{H}_s$, where $\mathcal{H}_a \cong \mathbb{C}^{2^k}$ denotes the Hilbert space of k ancillas. Then, for $\alpha \in \mathbb{R}^+$, the unitary operator U_A is called an (α, k)-*block-encoding* of A if for every state $|\psi\rangle \in \mathcal{H}_s$:

$$\left(\mathbb{1}_s \otimes \langle g|_g\right) U_A \left(\mathbb{1}_s \otimes |g\rangle_a\right) = A/\alpha\,, \tag{79}$$

where $|g\rangle_a$ is some state in $\mathcal{H}_a$, $\mathbb{1}_s$ is the identity operator on $\mathcal{H}_s$. The value α chosen such that $\|A\|/\alpha \leq 1$ is called the *scale factor* of the BE.

BEs can be constructed using LCU as follows

Lemma 8 (LCU block encoding)**.** *Let $U_0, \ldots, U_{M-1}$ be M unitary operators acting on a system Hilbert space $\mathcal{H}_s$ and define the operator $T = \sum_{i=0}^{M-1} \beta_i U_i$. The LCU method provides a $(\beta, \log M)$ BE of the operator T, where $\beta \equiv \sum_{i=0}^{M-1} \|\beta_i\|$. The gate complexity is given by $\mathcal{O}(M \log M)$ elementary gates.*

Proof. The proof of this Lemma can be found in many textbooks, see for example [49]. The asymptotic cost stems from the complexity of implementing the SELECT subroutine, since the cost of preparing an arbitrary state on $\log_2 M$ qubits in PREPARE is $\mathcal{O}(M)$ [58, 59], which is cheaper than the cost of SELECT, as we explain next. The gate complexity of SELECT is $\mathcal{O}(M \log M)$, which comes from sequentially implementing M unitaries, each being controlled on $k = \log M$ ancillary qubits. Decomposing k-controlled gates into elementary gates can be achieved at a cost linear in k, with the constant prefactor being smallest if k additional ancillary qubits are allowed to be used [32, 60]. For applications considered in this work, this gives a minor overhead in the qubit cost since k is logarithmic is the parameters of the system. □

Given a BE of the Hamiltonian, one can obtain an approximation to the time evolution operator using QSP.

Theorem 9 (QSP with Qubitization). *Let U_H be a an (α, k)-block-encoding of a Hamiltonian H acting on a Hilbert space $\mathcal{H}_s$. Furthermore, let t and ε be positive real values. Then there is a quantum circuit that produces a $\big(1 \pm \mathcal{O}(\varepsilon), k+2\big)$-block-encoding of the time evolution operator e^{-iHt} up to exponentiation error ε, and possesses a complexity of*

$$\mathcal{O}\big(\alpha t + \log(1/\varepsilon)\big)\,, \tag{80}$$

relative to the oracle U_H. The probability for this BE to succeed is

$$p > 1 - \mathcal{O}(\varepsilon)\,. \tag{81}$$

Proof. We will not prove this result rigorously, but point the reader to the pedagogical sections of this paper, with all statements made there having been rigorously proved in the literature [44]. The fact that the BE is $(\tilde{\alpha}, \tilde{k}) = (1 \pm \mathcal{O}(\varepsilon), k+2)$ can be easily understood. First, the BE of the time evolution operator requires two additional qubits, one ($|q\rangle$) for the qubitization and one ($|b\rangle$) to add the functional dependence on ϕ, giving $\tilde{k} = k+2$. The fact that $\tilde{\alpha} = 1 \pm \mathcal{O}(\varepsilon)$ follows from the fact that the operator we are block-encoding is a unitary operator, and our approximation is good up to error ε. Since the norm of a unitary operator is 1, this gives that both $\tilde{\alpha}$ and the success probability are unity (up to $\mathcal{O}(\varepsilon)$). □

3. HHKL

Theorem 10 (HHKL Algorithm). *Let Λ be a lattice of qubits embedded in d-dimensional Euclidean space of size L in each dimension, and let $\hat{H}$ be a geometrically-local Hamiltonian, normalized such that each local term has norm of order unity. Further, let $\tilde{t}$ and ε be positive real values. Then there exists an algorithm that approximates $\mathrm{e}^{-i\tilde{H}\tilde{t}}$ to exponentiation error ε, which requires*[14]

$$\mathcal{O}\left(\frac{L^{\mathsf{d}}\tilde{t}}{\log^{\mathsf{d}}\left(L^{\mathsf{d}}\tilde{t}/\varepsilon\right)}\right) \tag{82}$$

calls to a helper function that implements the time evolution of a system with

$$\ell = \Theta\Big(\log\left(L^{\mathsf{d}}\tilde{t}/\varepsilon\right)\Big)\,, \tag{83}$$

with error

$$\delta = \mathcal{O}\left(\frac{\varepsilon \log^{\mathsf{d}}(L^{\mathsf{d}}\tilde{t}/\varepsilon)}{L^{\mathsf{d}}\tilde{t}}\right) \tag{84}$$

Proof. The results follow directly from our discussion in Sec. II C. For formal proofs of the results stated there we refer the reader to the original paper [45]. □

4. QETU

Theorem 11 (QETU). *Let $U = \mathrm{e}^{-i\tau A}$ with an n-qubit Hermitian matrix A and real parameter τ. For any real even polynomial $F(x)$ with degree d satisfying $|F(x)| \le 1, \forall x \in [-1, 1]$, one can find a sequence of symmetric phase factors $(\varphi_0, \varphi_1, \ldots, \varphi_1, \varphi_0) \in \mathbb{R}^{d+1}$ such that the circuit in Fig. 7 denoted by $\mathcal{U}$ satisfies $(\langle 0| \otimes \mathbb{1})\mathcal{U}(|0\rangle \otimes \mathbb{1}) = F(\cos(\tau A/2))$.*

Proof. The proof of the QETU theorem can be found in Appendix B of Ref. [30]. □

III. SIMULATING TIME EVOLUTION ON THE LATTICE

In this section, we apply the algorithms and methods of Section II to the case of Hamiltonians defined in Sec. I B. Similar to Sec. II, this section is organized by the techniques used (PFs, QSP, and HHKL). For each of these sections, we begin by considering the case of $\mathcal{O}(1)$-site-local RHLFTs defined on $\mathcal{O}(1)$-many sites, which behave very similarly to generic quantum systems, and will serve as a review

[14] We assume that the error ε large enough that the number of calls to the helper function is larger than one.

of the relationship between our notation and other common notations. We then proceed to the case of k-site-local and k-geometrically-site-local Hamiltonians, whose simulation can roughly be categorized as being composed of simulation methods for $\mathcal{O}(1)$-site-local Hamiltonians that are "glued" via PFs, LCU, or HHKL, depending on the flavor of locality whose preservation is desired.

A. Product Formulas

Before we investigate the scaling of PFs for different local Hamiltonians with different numbers of lattice sites, we give two results that apply to all Hamiltonians considered in this work.

The general results on PFs depended on a parameter $\tilde{\alpha}$, which was related to the commutator of terms in the Hamiltonian. Our first Lemma relates this to the norm of the Hamiltonian

Lemma 12. *Let H be a k-site-local Hamiltonian, as defined in Definition 2. Then the nested commutator $\tilde{\alpha} \equiv \sum_{J_1,J_2,\dots,J_{p+1}\in S}||[H_{J_{p+1}},\dots[H_{J_2},J_{J_1}]]||$ can be asymptotically bounded as*

$$\tilde{\alpha} = \mathcal{O}\big(|||H|||_1^p ||H||_1\big)\,. \tag{85}$$

Proof. This result has been proven in Appendix G of [28]. □

The next Lemma will give an expression that will allow to combine a PF with another approximation to the exponentials that make up the PF. The PF introduced in Eq. (15) is used as an approximation to e^{-iHt}, and another approximation $U_\upsilon^{(J)}(t/r)$ is used to approximate each term of the form $\mathrm{e}^{-ita_\upsilon^{(J)}H_J/r}$.

Lemma 13. *Let H be a site-local Hamiltonian as defined by 2. Let $S_p(t)$ be a p^{th} order PF for e^{-iHt} as given in Eq. (15), and let the unitary $U_\upsilon^{(J)}(t/r)$ be an approximation to $\mathrm{e}^{-ita_\upsilon^{(J)}H_J/r}$ for all choices of allowed pairs (υ, J), with $\upsilon \in \{1,\dots,\Upsilon(p)\}$ and $J \in S$. Define the PF $\tilde{S}_p(t)$ as the PF for e^{-iHt} obtained by replacing $\mathrm{e}^{-ita_\upsilon^{(J)}H_J/r}$ in Eq. (15) with $U_\upsilon^{(J)}(t/r)$*

$$\tilde{S}_p(t/r) \equiv \prod_{\upsilon=1}^{\Upsilon} \mathcal{P}_\upsilon \prod_{J\in S} U^{(\upsilon,J)}(t/r)\,. \tag{86}$$

If

$$\left\|U_\upsilon^{(J)}(t/r) - \mathrm{e}^{-ita_\upsilon^{(J)}H_J/r}\right\| = \mathcal{O}\left(\frac{\varepsilon}{\mathsf{N_H} r}\right), \tag{87}$$

it is true that

$$\left\|\tilde{S}_p(t) - \mathrm{e}^{-iHt}\right\| = \mathcal{O}(\varepsilon)\,. \tag{88}$$

Proof. Demanding that the new PF still reproduces the time evolution operator with the same exponentiation error we can write

$$\begin{aligned}
&\left\|\mathrm{e}^{-iHt} - \tilde{S}_p(t)\right\| \\
&= \left\|\mathrm{e}^{-iHt} - S_p(t) + \big[S_p(t/r)\big]^r - \big[\tilde{S}_p(t/r)\big]^r\right\| \\
&\le \mathcal{O}(\varepsilon) + \left\|\big[\tilde{S}_p(t/r)\big]^r - \big[S_p(t/r)\big]^r\right\| \\
&= \mathcal{O}(\varepsilon) + r\,\mathsf{N_H}\left\|U_\upsilon^{(J)}(t/r) - \mathrm{e}^{-it/ra_{\upsilon J}H_J}\right\| \\
&= \mathcal{O}(\varepsilon)\,.
\end{aligned} \tag{89}$$

□

1. General site-local Hamiltonian

We can now give results that apply to both general site-local Hamiltonians (see Definition 2).

Theorem 14 (Product Formulas for site-local Hamiltonians)**.** *Let H be a site-local Hamiltonian as defined in Definition 2 or Definition 3. To simulate the time evolution operator e^{-iHt} up to exponentiation error $\mathcal{O}(\varepsilon)$ it suffices to choose a Trotter number r such that:*

$$r = \mathcal{O}\left(\mathsf{N_{ind}}\mathsf{N_H}^{1/p}\frac{(\mathsf{N_P c_P} t)^{1+\frac{1}{p}}}{\varepsilon^{\frac{1}{p}}}\right). \tag{90}$$

Furthermore, if the Trotter number r is chosen with tight the asymptotic scaling

$$r = \Theta\left(\mathsf{N_{ind}}\mathsf{N_H}^{1/p}\frac{(\mathsf{N_P c_P} t)^{1+\frac{1}{p}}}{\varepsilon^{\frac{1}{p}}}\right), \tag{91}$$

then the associated elementary gate count χ can be asymptotically bounded as

$$\chi = \mathcal{O}\left(\mathsf{N_{ind}}\mathsf{N_P}\frac{(\mathsf{N_H N_P c_P} t)^{1+\frac{1}{p}}}{\varepsilon^{\frac{1}{p}}}\right). \tag{92}$$

Proof. Using Theorem 6 and Lemma 12one finds that the Trotter number r is given by

$$r = \mathcal{O}\left(\frac{|||H|||_1||H||_1^{\frac{1}{p}}t^{1+\frac{1}{p}}}{\varepsilon^{\frac{1}{p}}}\right). \tag{93}$$

Using previously established notation, we have

$$\begin{aligned}
||H||_1 &= \mathcal{O}\left(\mathsf{N_H}\sum_J ||H_J||\right) = \mathcal{O}(\mathsf{N_H N_P c_P})\,, \\
|||H|||_1 &= \mathcal{O}(\mathsf{N_{ind} N_P c_P})\,,
\end{aligned} \tag{94}$$

which immediately gives

$$r=\mathcal{O}\left(\mathsf{N_{ind}}\mathsf{N_H}^{1/p}\frac{(\mathsf{N_P c_P}t)^{1+\frac{1}{p}}}{\varepsilon^{\frac{1}{p}}}\right). \tag{95}$$

Assume now that we wish to compute the total gate count χ for a quantum circuit implementing an approximation of e^{-iHt} to total exponentiation error $\mathcal{O}(\varepsilon)$ based on the splitting $\left(S_p(t/r)\right)^r$, where the Trotter number r in fact satisfies (91) (i.e., the asymptotic scaling is tight) so that the spectral norm $\|\left(S_p(t/r)\right)^r-\mathrm{e}^{-iHt}\|=\mathcal{O}(\varepsilon)$. This splitting takes the following form (see Eq. (15))

$$\left[S_p(t/r)\right]^r\equiv\left(\prod_{\upsilon=1}^{\Upsilon(p)}\mathcal{P}_\upsilon\left(\prod_{J\in S}\exp\left(\frac{-ita_\upsilon^{(J)}H_J}{r}\right)\right)\right)^r. \tag{96}$$

Each $S_p(t/r)$ thus consists of $\mathcal{O}\left(\mathsf{N_H}\Upsilon(p)\right)$-many exponentials of the form $\exp\left(-ita_\upsilon^{(J)}H_J/r\right)$. Each of these exponentials can be approximated using a different PF $\tilde{S}_{\tilde{p}}^{(\upsilon,J)}(t/r\tilde{r})$ based on the Pauli decomposition of each term H_J (see Eq. (3)). This splitting takes the form

$$\begin{aligned}&\left[\tilde{S}_{\tilde{p}}^{(\upsilon,J)}(t/(r\tilde{r}))\right]^{\tilde{r}}\\&\equiv\left(\prod_{\upsilon=1}^{\Upsilon(\tilde{p})}\tilde{\mathcal{P}}_\upsilon\left(\prod_{i=1}^{\mathsf{N_P}^{(J)}}\exp\left(\frac{-it\tilde{a}_\upsilon^{(i)}c_i^{(J)}P_i^{(J)}}{r\tilde{r}}\right)\right)\right)^{\tilde{r}}.\end{aligned} \tag{97}$$

From Lemma 13 we know that to ensure that the total error remains $\mathcal{O}(\varepsilon)$, the accuracy of this PF has to be

$$\begin{aligned}&\left\|\left(\tilde{S}_{\tilde{p}}^{(\upsilon,J)}(t/r\tilde{r})\right)^{\tilde{r}}-\exp\left(\frac{-ita_\upsilon^{(J)}H_J}{r}\right)\right\|\\&=\mathcal{O}\left(\frac{\varepsilon}{\mathsf{N_H}r\Upsilon(p)}\right).\end{aligned} \tag{98}$$

Substituting this into the result of Theorem 6 we therefore find

$$\begin{aligned}\tilde{r}&=\Omega\left(\left(\frac{\mathsf{N_P c_P}t}{r}\right)^{1+\frac{1}{\tilde{p}}}\left(\frac{\varepsilon}{\mathsf{N_H}\Upsilon(p)r}\right)^{-\frac{1}{\tilde{p}}}\right)\\&=\Omega\left(\frac{\Upsilon(p)}{\mathsf{N_{ind}}}\left(\frac{\mathsf{N_P c_P}t}{\mathsf{N_H}\varepsilon}\right)^{\frac{p}{\tilde{p}}}\right).\end{aligned} \tag{99}$$

We choose $\tilde{p}=p$ and use that both $\Upsilon(p)$ and $\Upsilon(\tilde{p})=\mathcal{O}(1)$. We also have that $\tilde{r},\mathsf{N_{ind}}\in\mathbb{N}$ have to both be at least 1, and hence one finds $\tilde{r}=\Omega(1)$.

The resource scaling is thus given by

$$\begin{aligned}\chi&=\mathcal{O}(\mathsf{N_H N_P}r)\\&=\mathcal{O}\left(\mathsf{N_{ind}N_P}\frac{(\mathsf{N_H N_P c_P}t)^{1+\frac{1}{p}}}{\varepsilon^{\frac{1}{p}}}\right).\end{aligned} \tag{100}$$

□

2. $\mathcal{O}(1)$ site-local Hamiltonian

Having obtained the results for a general site-local Hamiltonian, one can obtain the results for an $\mathcal{O}(1)$ site-local Hamiltonian

Theorem 15 (Product Formulas for $\mathsf{N_\Lambda}=\mathcal{O}(1)$ sites)**.** *Let H be an $\mathcal{O}(1)$ Hamiltonian as defined in Definition 4 Let $S_p(t)$ be a p^{th} order PF as given by Eq.* (15) *and Eq.* (77)*. Then to simulate the time evolution operator e^{-iHt} up to exponentiation error $\mathcal{O}(\varepsilon)$ it suffices to choose a Trotter number r such that:*

$$r=\mathcal{O}\left(\frac{(\mathsf{N_P c_P}t)^{1+\frac{1}{p}}}{\varepsilon^{\frac{1}{p}}}\right). \tag{101}$$

Furthermore, if the Trotter number r is chosen with the tight asymptotic scaling

$$r=\Theta\left(\frac{(\mathsf{N_P c_P}t)^{1+\frac{1}{p}}}{\varepsilon^{\frac{1}{p}}}\right), \tag{102}$$

then the associated elementary gate count χ can be asymptotically bounded as

$$\chi=\mathcal{O}\left(\frac{\mathsf{N_P}\left(\mathsf{N_P c_P}t\right)^{1+\frac{1}{p}}}{\varepsilon^{\frac{1}{p}}}\right). \tag{103}$$

Proof. This result is obtained immediately by setting $\mathsf{N_H}\sim\mathsf{N_{ind}}=\mathcal{O}(1)$ in Theorem 14. □

3. Geometrically-site-local Hamiltonian

Theorem 16 (Product Formulas for geometrically-site-local Hamiltonians)**.** *Let H be a geometrically site-local Hamiltonian as defined in Definition 3. To simulate the time evolution operator e^{-iHt} up to exponentiation error $\mathcal{O}(\varepsilon)$ it suffices to choose a Trotter number r such that:*

$$r=\mathcal{O}\left(\mathsf{N_\Lambda}^{1/p}\frac{(\mathsf{N_P c_P}t)^{1+\frac{1}{p}}}{\varepsilon^{\frac{1}{p}}}\right). \tag{104}$$

Furthermore, if the Trotter number r is chosen with tight the asymptotic scaling

$$r = \Theta\left(\mathsf{N}_\Lambda{}^{1/p} \frac{(\mathsf{N}_\mathsf{P} \mathsf{c}_\mathsf{P} t)^{1+\frac{1}{p}}}{\varepsilon^{\frac{1}{p}}} \right), \tag{105}$$

then the associated elementary gate count χ can be asymptotically bounded as

$$\chi = \mathcal{O}\left(\mathsf{N}_\mathsf{P} \frac{(\mathsf{N}_\Lambda \mathsf{N}_\mathsf{P} \mathsf{c}_\mathsf{P} t)^{1+\frac{1}{p}}}{\varepsilon^{\frac{1}{p}}} \right). \tag{106}$$

Proof. This result follows directly from Theorem 14 making the replacements $\mathsf{N}_\mathsf{ind} = \mathcal{O}(1)$ and $\mathsf{N}_\mathsf{H} = \mathcal{O}(\mathsf{N}_\Lambda)$ as given in Eqs. (12) and (13). □

B. Quantum Signal Processing

As discussed in detail in Sec. II E 2, QSP provides a technique to take the BE of a given Hamiltonian and obtain the approximation to the BE of its time evolution operator. We will begin by deriving the general result of using QSP to implement the time evolution operator of the full system Hamiltonian.

We will also derive results that combine the techniques of PFs with those of QSP. In this approach we will use a PF to split the full time evolution operator into products of exponentials of the form $\mathrm{e}^{-ita_v^{(J)} H_J/r}$, and then use QSP to to obtain expression for these exponentials requiring only $\mathcal{O}(1)$ lattice sites.

In both of these approaches we assume that the original BE is achieved using LCU, as explained in Sec. II B 2, but we note that other techniques are possible as well.

1. General site-local Hamiltonian

We first establish the scaling of the LCU that will be used for the BE

Lemma 17 (LCU for site-local Hamiltonians)**.** *Let H be a site-local Hamiltonian as as in Definition 2. There exists a quantum circuit acting on $\mathsf{n} \equiv \mathsf{N}_\Lambda \mathsf{n}_\mathsf{q}$-many qubits together with $k = \mathcal{O}\left(\log(\mathsf{N}_\mathsf{H}\mathsf{N}_\mathsf{P})\right)$-many ancillas that produces an $\left(\mathcal{O}\left(\mathsf{N}_\mathsf{H}\mathsf{N}_\mathsf{P}\mathsf{c}_\mathsf{P}\right), k\right)$-block-encoding of H on the n qubits, and requires a total of $\mathcal{O}\left(\mathsf{N}_\mathsf{H}\mathsf{N}_\mathsf{P}\log(\mathsf{N}_\mathsf{H}\mathsf{N}_\mathsf{P})\right)$-many elementary quantum gates.*

Proof. This follows directly from Lemma 8, if we observe that the total number of Pauli strings is given by $\mathsf{N}_\mathsf{H}\mathsf{N}_\mathsf{P}$ and the sum of the coefficients of all Pauli strings is bounded by $\beta < \mathsf{N}_\mathsf{H}\mathsf{N}_\mathsf{P}$. □

Given this result now allows us to state the central QSP result we use in this work:

Theorem 18 (QSP for site-local Hamiltonians)**.** *Let H be a site-local Hamiltonian as defined by 2, and let t and ε be positive values. Then there exists a quantum circuit that serves as a $\left(1 \pm \mathcal{O}(\varepsilon), \mathcal{O}(\log(\mathsf{N}_\mathsf{H}\mathsf{N}_\mathsf{P}))\right)$-block-encoding for e^{-iHt} up to exponentiation error ε, and requires an elementary gate count of*

$$\chi = \mathcal{O}\Big[\mathsf{N}_\mathsf{H}\mathsf{N}_\mathsf{P}\log(\mathsf{N}_\mathsf{H}\mathsf{N}_\mathsf{P})\left(\mathsf{N}_\mathsf{H}\mathsf{N}_\mathsf{P}\mathsf{c}_\mathsf{P} t + \log(1/\varepsilon)\right)\Big]. \tag{107}$$

Proof. This result follows from Lemma 17 and Theorem 9. From Lemma 17 one obtains that LCU give a $\Big(\mathcal{O}\left(\mathsf{N}_\mathsf{H}\mathsf{N}_\mathsf{P}\mathsf{c}_\mathsf{P}\right), \mathcal{O}\left(\log(\mathsf{N}_\mathsf{H}\mathsf{N}_\mathsf{P})\right)\Big)$ BE of the Hamiltonian. Using this result in Theorem 9 one finds that QSP gives a $\left(1 \pm \mathcal{O}(\varepsilon), \mathcal{O}(\log(\mathsf{N}_\mathsf{H}\mathsf{N}_\mathsf{P}))\right)$-block-encoding for e^{-iHt}. Using the resource scaling from Theorem 9, with the scale factor and resource scaling of LCU from Lemma 17, gives the resource requirements stated in the theorem. □

Remark 19. Note that we have assumed that the block-encoding is formed from a sum over all Pauli strings appearing in the Hamiltonian. When more structure is known about a given field theory, the factor in the complexity due to the block-encoding may be reduced.

2. $\mathcal{O}(1)$ site-local Hamiltonian

As for the PF, we can obtain the QSP requirements of an $\mathcal{O}(1)$ site-local Hamiltonian:

Theorem 20 (QSP for $\mathcal{O}(1)$ sites)**.** *Let H be an $\mathcal{O}(1)$ Hamiltonian as defined in Definition 4, and let t and ε be positive values. Then there exists a quantum circuit that serves as a $\left(1 \pm \mathcal{O}(\varepsilon), \mathcal{O}(\log(\mathsf{N}_\mathsf{P}))\right)$-block-encoding for e^{-iHt} up to exponentiation error ε, and requires an elementary gate count of*

$$\chi = \mathcal{O}\Big[\mathsf{N}_\mathsf{P}\log\mathsf{N}_\mathsf{P}\left(\mathsf{N}_\mathsf{P}\mathsf{c}_\mathsf{P} t + \log(1/\varepsilon)\right)\Big]. \tag{108}$$

Proof. This follows directly from Theorem 18 by taking the limit $\mathsf{N}_\mathsf{H} = \mathcal{O}(1)$. □

3. Geometrically-site-local Hamiltonian

Theorem 21 (QSP for geometrically-site-local Hamiltonians)**.** *Let H be a geometrically site-local Hamiltonian as defined by 2, and let t and ε be positive values. Then there exists a quantum circuit that* *serves as a* $\left(1\pm\mathcal{O}(\varepsilon),\mathcal{O}(\log(\mathsf{N_H N_P}))\right)$*-block-encoding for* e^{-iHt} *up to exponentiation error* ε*, and requires an elementary gate count of*

$$\chi=\mathcal{O}\Big[\mathsf{N_\Lambda N_P}\log(\mathsf{N_\Lambda N_P})\left(\mathsf{N_\Lambda N_P c_P}t+\log(1/\varepsilon)\right)\Big]. \tag{109}$$

Proof. This result follows directly from Theorem 18 making the replacements $\mathsf{N_H}=\mathcal{O}(\mathsf{N_\Lambda})$ as given in Eq. (13). □

C. Combining Product Formula with QSP

In this section we consider combining a PF with QSP. We will use Lemma 13 to write a PF for e^{-iHt}, but then use QSP for $U^{(v,J)}(t/r)$, which serves as an approximation to $\mathrm{e}^{-it/ra_{vJ}H_J}$ in the PF.

Theorem 22 (QSP applied to Product Formulas)**.** *Let* H *be a site-local Hamiltonian as defined by 2, and let* t *and* ε *be positive values. By using QSP (see Theorem 20) to simulate each exponential term* $\mathrm{e}^{-ia_v^{(J)}H_J t/r}$ *appearing in the PF* $S_p(t/r)$ *to error* $\varepsilon/(r\mathsf{N_H})$*, and taking*

$$r=\Theta\left(\mathsf{N_{ind}}\mathsf{N_H}^{1/p}\frac{(\mathsf{N_P c_P}t)^{1+\frac{1}{p}}}{\varepsilon^{\frac{1}{p}}}\right), \tag{110}$$

we obtain a quantum circuit that serves as a $(1\pm\mathcal{O}(\varepsilon),\log(\mathsf{N_H N_P}))$*-block-encoding for the full time evolution operator* e^{-iHt} *to exponentiation error* $\mathcal{O}(\varepsilon)$*. The gate count for this circuit is given by*

$$\chi=\mathcal{O}\Big[\mathsf{N_{ind}}\left(\mathsf{N_H N_P c_P}t\right)^{1+\frac{1}{p}}\varepsilon^{-\frac{1}{p}}\mathsf{N_P}\log\mathsf{N_P} \\ \times\log(\mathsf{N_{ind}N_H N_P c_P}t/\varepsilon)\Big]. \tag{111}$$

Proof. From Lemma 13 we know that the simulation of a single exponential of the form $\mathrm{e}^{-ia_v^{(J)}H_J t/r}$ acting on $\mathcal{O}(1)$ sites is needed to accuracy $\varepsilon/(\mathsf{N_H}r)$. Performing this approximation using QSP (see Theorem 20) requires a gate count

$$\chi_J=\mathcal{O}\left(\mathsf{N_P}\log\mathsf{N_P}\left(\mathsf{N_P c_P}\frac{t}{r}+\log(\mathsf{N_H}r/\varepsilon)\right)\right) \\ =\mathcal{O}\left(\mathsf{N_P}\log\mathsf{N_P}\log(\mathsf{N_H}r/\varepsilon)\right), \tag{112}$$

where the first term can be discarded because the asymptotic assumption on r given by (110) indicates that $\mathsf{N_P c_P}t/r=\mathcal{O}(\varepsilon/(\mathsf{N_P c_P}t)^{1/p})$, which is asymptotically bounded from above by a constant.

The total gate count from the $(\mathsf{N_H}r)$-many applications of this QSP subroutine is then given by

$$\chi=\mathsf{N_H}\,r\,\chi_J \\ =\mathcal{O}\Big[\mathsf{N_{ind}}\left(\mathsf{N_H N_P c_P}t\right)^{1+\frac{1}{p}}\varepsilon^{-\frac{1}{p}} \\ \times\mathsf{N_P}\log\mathsf{N_P}\log(\mathsf{N_{ind}N_H N_P c_P}t/\varepsilon)\Big]. \tag{113}$$

Since the block-encoding produced by QSP has a scale factor $1\pm\mathcal{O}(\varepsilon/(r\mathsf{N_H}))$, the final block-encoding produced by multiplying $(\Upsilon(p)\mathsf{N_H}r)$-many such block-encodings will again be a block-encoding, this time with scale-factor $1\pm\mathcal{O}(\varepsilon)$. This completes the proof. □

Remark 23. The results above were for a general site-local Hamiltonian. To obtain the results for a geometrically site-local Hamiltonian one makes the replacement $\mathsf{N_{ind}}=\mathcal{O}(1)$ and $\mathsf{N_H}=\mathcal{O}(\mathsf{N_\Lambda})$ from Eqs. (12) and (13).

D. HHKL

As discussed in Sec. II C the HHKL technique is a method of "gluing" together implementations of a time evolution operator on a "local" lattice with size ℓ^{d}. In this section we consider HHKL with two approaches for the implementation of the local evolution operator, first using a PF and then QSP.

Theorem 24 (HHKL with PF as helper)**.** *Let* H *be a geometrically site-local Hamiltonian as defined by 3, and let* t *and* ε *be positive values. Using the HHKL algorithm with a PF for the helper function gives rise to an algorithm that approximates the time evolution operator* e^{-iHt} *with exponentiation error requiring a gate complexity of*

$$\chi=\mathsf{N_P}\left(\mathsf{N_\Lambda N_P c_P}t\right)^{1+\frac{1}{p}}\varepsilon^{-\frac{1}{p}}. \tag{114}$$

Proof. From Theorem 10 we need the helper function to implement a time evolution operator for time $\tilde{t}=\|H_J\|t=\mathcal{O}(\mathsf{N_P c_P}t)$ on a system of size $N_\ell=\mathcal{O}(\ell^d)$ with exponentiation error δ, where ℓ and δ are given in Eqs. (83) and (84).

From Theorem 14 we find that a PF to implement the time evolution on a system with N_ℓ lattice sites and exponentiation error δ requires resources (taking

$t = \mathcal{O}(1)$ in Eq. (107))

$$\begin{aligned}\chi_{\rm PF} &= \mathcal{O}\Big(\mathsf{N_P}\left(\mathsf{N}_\ell \mathsf{N_P c_P}\right)^{1+\frac{1}{p}} \delta^{-\frac{1}{p}}\Big) \\ &= \mathcal{O}\Bigg(\mathsf{N_P}\left(\mathsf{N_P c_P}\right)^{1+\frac{1}{p}} \Big[\log\left(\mathsf{N_\Lambda} t/\varepsilon\right)\Big]^{\mathsf{d}\left(1+\frac{1}{p}\right)} \\ &\qquad \times \left(\frac{\mathsf{N_\Lambda} t}{\varepsilon \log^d\left(\mathsf{N_\Lambda} t/\varepsilon\right)}\right)^{\frac{1}{p}}\Bigg) \\ &= \mathcal{O}\left(\mathsf{N_P}\left(\mathsf{N_P c_P}\right)^{1+\frac{1}{p}} \log^{\mathsf{d}}\left(\frac{\mathsf{N_\Lambda} t}{\varepsilon}\right)\left(\frac{\mathsf{N_\Lambda} t}{\varepsilon}\right)^{\frac{1}{p}}\right).\end{aligned} \tag{115}$$

Furthermore, we know from Theorem 10 that the number of calls to this helper function is given by Eq. (82), such that the final gate complexity is

$$\begin{aligned}\chi &= \mathcal{O}\left(\frac{\mathsf{N_\Lambda} t}{\log^{\mathsf{d}}\left(\mathsf{N_\Lambda} t/\varepsilon\right)}\chi_{\rm PF}\right) \\ &= \mathcal{O}\Big(\mathsf{N_P}\left(\mathsf{N_\Lambda N_P c_P} t\right)^{1+\frac{1}{p}} \varepsilon^{-\frac{1}{p}}\Big).\end{aligned} \tag{116}$$

as desired. □

Theorem 25 (HHKL with QSP as helper)**.** *Let H be a geometrically site-local Hamiltonian as given by Definition 3, and let t and ε be positive values. Using the HHKL algorithm with QSP for the helper function gives rise to an algorithm that approximates the time evolution operator e^{-iHt} with exponentiation error requiring a gate complexity of*

$$\chi = \mathcal{O}\Big(\mathsf{N_P}^2 \mathsf{N_\Lambda c_P} t \log^{\mathsf{d}}\left(\mathsf{N_\Lambda} t/\varepsilon\right) \log\Big(\mathsf{N_P} \log\left(\mathsf{N_\Lambda} t/\varepsilon\right)\Big)\Big). \tag{117}$$

Proof. Theorem 10 states that we need the helper function to implement a time evolution operator for time $\tilde{t} = \|H_J\| t = \mathcal{O}(\mathsf{N_P c_P} t)$ on a system of size $N_\ell = \mathcal{O}(\ell^d)$ with exponentiation error δ, where ℓ and δ are given in Eqs. (83) and (84). From Theorem 18 we find that implementing the time evolution on a system with N_ℓ lattice sites and exponentiation error δ with QSP requires resources (taking $t = \mathcal{O}(1)$ in Eq. (107))

$$\begin{aligned}\chi_{\rm QSP} &= \mathcal{O}\Big(\mathsf{N}_\ell \mathsf{N_P} \log\left(\mathsf{N}_\ell \mathsf{N_P}\right)\left(\mathsf{N}_\ell \mathsf{N_P c_P} + \log(1/\delta)\right)\Big] \\ &= \mathcal{O}\Bigg(\log^{\mathsf{d}}\left(\mathsf{N_\Lambda} t/\varepsilon\right) \mathsf{N_P} \log\Big[\mathsf{N_P} \log\left(\mathsf{N_\Lambda} t/\varepsilon\right)\Big] \\ &\qquad \times \Bigg[\mathsf{N_P c_P} \log^{\mathsf{d}}\left(\mathsf{N_\Lambda} t/\varepsilon\right) \\ &\qquad\qquad + \log\left(\frac{\mathsf{N_\Lambda} t}{\varepsilon \log^{\mathsf{d}}\left(\mathsf{N_\Lambda} t/\varepsilon\right)}\right)\Bigg]\Bigg).\end{aligned} \tag{118}$$

In the limit of large system size, the second term in the last square bracket (the one originating from the $\log(1/\delta)$ term) is subdominant to the first, which allows us to write

$$\chi_{\rm QSP} = \mathcal{O}\Big(\mathsf{N_P c_P} \log^{2\mathsf{d}}\left(\mathsf{N_\Lambda} t/\varepsilon\right) \log\Big[\mathsf{N_P} \log\left(\mathsf{N_\Lambda} t/\varepsilon\right)\Big]\Big). \tag{119}$$

Using the number of calls to this helper function from Eq. (82), the final gate complexity is

$$\begin{aligned}\chi &= \mathcal{O}\left(\frac{\mathsf{N_\Lambda} t}{\log^{\mathsf{d}}\left(\mathsf{N_\Lambda} t/\varepsilon\right)}\chi_{\rm QSP}\right) \\ &= \mathcal{O}\Big(\mathsf{N_P}^2 \mathsf{N_\Lambda c_P} t \log^{\mathsf{d}}\left(\mathsf{N_\Lambda} t/\varepsilon\right) \log\Big[\mathsf{N_P} \log\left(\mathsf{N_\Lambda} t/\varepsilon\right)\Big]\Big),\end{aligned} \tag{120}$$

as desired. □

IV. LATTICE QUARTIC THEORY

The results we have discussed so far are theoretical worst-case asymptotic complexities, applicable to any lattice field theory with prescribed locality properties. In this section, we specialize to a particular model of interacting quantum field theories: the lattice scalar field theory. From the computational perspective, this theory is similar to lattice gauge theories and so intuition can be drawn from its consideration. Furthermore, it is often used as a proverbial example in the studies of quantum simulation algorithms [9, 15, 19], and so detailed comparisons with past work can be performed.

In this section, we review the Hamiltonian of the theory and our procedure for digitizating the bosonic field. Throughout the discussion, we will keep track of the parameters of the theory required for quoting the asymptotic gate complexities derived in Sec. III, e.g., $\mathsf{N_P}$, $\mathsf{c_P}$, $\mathsf{N_H}$, etc. We then determine the asymptotic gate complexities for implementing time-evolution using PFs, QSP with several different BE methods, and the HHKL algorithm.

A. Introduction

The model we consider is defined on a hypercubic lattice Λ of spatial dimension d with lattice spacing a. Assuming the simplest finite-difference approximation to the spatial derivative $(\nabla_\mu \hat{\varphi})^2$, the Hamiltonian is given by[15]

$$\hat{H}_{\text{quartic}} = \hat{H}_\varphi + \hat{H}_\pi \,, \tag{121a}$$

$$\hat{H}_\varphi = a^{\mathsf{d}} \left[\sum_{i=1}^{\mathsf{N}_\Lambda} \frac{m}{2}\hat{\varphi}_i^2 + \frac{\lambda}{4!}\hat{\varphi}_i^4 + \sum_{\langle ij \rangle} \frac{(\hat{\varphi}_j - \hat{\varphi}_i)^2}{2a^2} \right], \tag{121b}$$

$$\hat{H}_\pi = a^{\mathsf{d}} \sum_{i=1}^{\mathsf{N}_\Lambda} \frac{1}{2}\hat{\pi}_i^2 \,, \tag{121c}$$

where and the indices i and j label lattice sites, and the notation $\langle ij \rangle$ runs over all distinct links joining nearest neighbors in the lattice. In the remainder of this work, we will denote operators with a hat to differentiate between their digitized eigenvalues.

The Hamiltonian in Eq. (121) is 2-site-geometrically-local, which implies that $\mathsf{N}_{\mathsf{ind}} = \mathcal{O}(1)$. We see that the Hamiltonian is a sum of $\mathsf{N}_{\mathsf{H}} = \mathcal{O}(\mathsf{N}_\Lambda)$ terms.

The operators $\hat{\pi}_i$ and $\hat{\varphi}_i$ are conjugate operators satisfying $[\hat{\varphi}_j, \hat{\pi}_i] = ia^{-\mathsf{d}}\delta_{ij}$. This relation implies that the so-called field basis, in which the φ_i operators are diagonal, is related to the so-called momentum basis, where the π_i operators are diagonal, by the usual Fourier transform. The parameters m and λ are bare quantities, and are in general complicated non-perturbative functions of the lattice spacing, *i.e.* $m = m(a)$ and $\lambda = \lambda(a)$. In principle, this functional dependence could be included to determine the asymptotic complexity of a realistic physical calculation in terms of the lattice spacing. In order to keep our expressions as general as possible, however, we choose to leave the bare parameters m and λ as free variables in our quoted asymptotic complexities; this allows our results to be adapted in a straightforward way to any specific physical use case. For the remainder of this work, we use units where the lattice spacing $a = 1$.

The above Hamiltonian, although discretized on the lattice, is still an unbounded operator acting on an infinite dimensional Hilbert space. In order to obtain concrete time-evolution operators whose action can actually be simulated on a system of qubits, we must first truncate this Hamiltonian to a finite-dimensional operator. This is achieved by a procedure known as *digitization*, in which the Hilbert space at each lattice site is represented using $\mathsf{n_q}$ qubits; the details of our digitization procedure are given in the next section.

[15] The following discussion can be generalized to the case of higher-order finite-difference approximations to the derivative operator.

1. Digitization

The basic idea is that we wish to construct a sequence of matrix operators $H_{\mathsf{n_q}}$ that can act on $\mathsf{n_q}$ qubits at a time, and whose spectrum converges to any prescribed single-site Hamiltonian H as $\mathsf{n_q} \to \infty$. There are numerous ways to proceed with such a construction [61–63], but the one we follow is outlined in [11].

The strategy is to *digitize* the field on a given lattice site into $N = 2^{\mathsf{n_q}}$ allowed field values

$$\varphi \in \{-\varphi_{\max}, -\varphi_{\max} + \delta\varphi, \ldots, \varphi_{\max} - \delta\varphi, \varphi_{\max}\} \,, \tag{122}$$

where the spacing $\delta\varphi$ is given by

$$\delta\varphi = \frac{2\varphi_{\max}}{N-1} \,. \tag{123}$$

This restriction of the field values is to be understood as a restriction of the Hilbert space at the given lattice site, identifying the eigenvalues of the restricted field operator precisely with this set of allowed field values. In other words, the digitized field operator in the field basis at site i becomes the diagonal matrix

$$\hat{\varphi}_i = \operatorname{diag}\left(\varphi_{\min}, \varphi_{\min} + \delta\varphi, \ldots, \varphi_{\max}\right)_i \,. \tag{124}$$

This single-site field operator acts nontrivially only on the $\mathsf{n_q}$-qubit Hilbert space attributed to the site labeled by i. Note that all lattice sites use the same digitized φ values.

Because $\hat{\pi}_i$ and $\hat{\varphi}_i$ are conjugate operators, the momentum operator in the field basis can be written as

$$\begin{aligned} \hat{\pi}_i &= \mathrm{FT} \cdot \hat{\pi}_i^{(p)} \cdot \mathrm{FT}^{-1} \,, \\ \hat{\pi}_i^{(p)} &= \operatorname{diag}\left(-\pi_{\max}, -\pi_{\max} + \delta\pi, \ldots, \pi_{\max}\right)_i \,, \end{aligned} \tag{125}$$

where the superscript (p) indicates the operator is represented in the momentum basis, FT denotes the *symmetric Fourier transform* [11] and

$$\pi_{\max} = \frac{\pi}{\delta\varphi}, \quad \delta\pi = \frac{2\pi_{\max}}{N-1} \,. \tag{126}$$

Note that this choice implies anti-periodic boundary conditions in field space. Using this definition, the momentum part of the Hamiltonian can be written as

$$\hat{H}_\pi = \sum_{i=1}^{\mathsf{N}_\Lambda} \frac{1}{2} \mathrm{FT}_i \cdot \left(\hat{\pi}_i^{(p)}\right)^2 \cdot \mathrm{FT}_i^{-1} \,. \tag{127}$$

The final component of the digitization strategy is the choice of $\varphi_{\max}$. It was shown in Ref. [11] that, for a given value of $\mathsf{n_q}$ and λ, there is an optimal choice of $\varphi_{\max}$ that minimizes the digitization error of the low lying spectrum of the digitized Hamiltonian. The procedure for determining $\varphi_{\max}$ involved scanning over many values to minimize the digitization error. While this procedure is in general possible, an explicit formula for the optimal value of $\varphi_{\max}$ for the $\lambda = 0$ case was given in Refs. [61, 63, 64]. As argued in Ref. [11], because $\lambda \neq 0$ results in a smooth deformation of the wavefunction, this choice of $\varphi_{\max}$ is expected to work well even in the $\lambda \neq 0$ case. Therefore, we use the value

$$\varphi_{\max} = 2^{\mathsf{n_q}} \sqrt{\frac{2\pi}{2^{\mathsf{n_q}+1}+1}}\,, \tag{128}$$

as in [38].

Altogether, these definitions allow for the construction of $2^{\mathsf{n_q}} \times 2^{\mathsf{n_q}}$ Hermitian matrices that digitize each of the single-site terms in Hamiltonian (121) into operators that can act on $\mathsf{n_q}$ qubits at a time. An appropriate full digitization of Hamiltonian (121) is then obtained by directly substituting the definitions of the digitized single-site operators $\hat{\varphi}_i$ and $\hat{\pi}_i$ into (121), together with the link terms $\hat{\varphi}_i\hat{\varphi}_j = \hat{\varphi}_i \otimes \hat{\varphi}_j$.

We are now in a position to discuss the parameters of this theory necessary for determining the cost of the various methods described in Sec.II E. Recall that we found $\mathsf{N_H} = \mathcal{O}(\mathsf{N_\Lambda})$ and $\mathsf{N_{ind}} = \mathcal{O}(1)$. The final parameters needed are $\mathsf{N_P}$ and $\mathsf{c_P}$, which we now discuss.

To determine the maximum number of Pauli strings $\mathsf{N_P}$ appearing in any term in $\hat{H}$, we start by writing the various operators in terms of Pauli operators. Note that the $\mathsf{n_q}$ qubit operators $\hat{\varphi}_i$ and $\hat{\pi}_i^{(p)}$ are diagonal operators with evenly spaced eigenvalues. It was shown in Ref. [11] that operators of this form can be decomposed into $\mathsf{n_q}$ single Pauli-Z gates. For example, one has $\hat{\varphi} = \frac{\varphi_{\max}}{2^{\mathsf{n_q}}-1}\sum_{j=0}^{\mathsf{n_q}-1} 2^j Z_j$, where Z_j is a single Pauli-Z gate acting on qubit j. Using this relation, we see that $\mathsf{N_P}$ for the various terms in H_φ are

$$\mathsf{N_P}^{(\varphi_i^2)} = \mathcal{O}({\mathsf{n_q}}^2)\,, \tag{129a}$$

$$\mathsf{N_P}^{(\varphi_i^4)} = \mathcal{O}({\mathsf{n_q}}^4)\,, \tag{129b}$$

$$\mathsf{N_P}^{(\varphi_i\varphi_j)} = \mathcal{O}({\mathsf{n_q}}^2)\,. \tag{129c}$$

Turning now to $\hat{H}_\pi$, while the operator $(\hat{\pi}_i^{(p)})^2$ is a sum of $\mathcal{O}({\mathsf{n_q}}^2)$ gates, the same is not true for $\hat{\pi}_i^2 = \mathrm{FT}\cdot(\hat{\pi}_i^{(p)})\cdot\mathrm{FT}^\dagger$; after using the Fourier transform to change to the field basis, the operator $\hat{\pi}_i^2$ is dense and requires $\mathcal{O}(4^{\mathsf{n_q}})$ Pauli strings. Because the quantum Fourier transform requires $\mathcal{O}({\mathsf{n_q}}^2)$ gates, it is more cost effective to first decompose $(\hat{\pi}_i^{(p)})^2$ into $\mathcal{O}({\mathsf{n_q}}^2)$ Pauli strings, and then change to the field basis using the Fourier transform. Using this method results in

$$\mathsf{N_P}^{(\pi^2)} = \mathcal{O}({\mathsf{n_q}}^2)\,. \tag{130}$$

From this we see that $\mathsf{N_P}$ for the entire Hamiltonian is dominated by the $\hat{\varphi}^4$ term, and is given by

$$\mathsf{N_P} = \mathcal{O}({\mathsf{n_q}}^4)\,. \tag{131}$$

This result for $\mathsf{N_P}$ is significantly more favorable than the worst case scaling for an arbitrary 2-site-local Hamiltonian of $\mathcal{O}(4^{2\mathsf{n_q}})$.

The final piece is to determine the maximum coefficient $\mathsf{c_P}$ of any Pauli string in $\hat{H}$. Using the fact that our choice of digitization leads to $\pi_{\max} = \mathcal{O}(2^{\mathsf{n_q}/2})$ and $\varphi_{\max} = \mathcal{O}(2^{\mathsf{n_q}/2})$, we see

$$\mathsf{c_P}^{(\pi^2)} = \mathcal{O}(\pi_{\max}^2) = \mathcal{O}(2^{\mathsf{n_q}}), \tag{132}$$

$$\mathsf{c_P}^{(\varphi^2)} = \mathcal{O}(m^2\varphi_{\max}^2) = \mathcal{O}(m^2 2^{\mathsf{n_q}}), \tag{133}$$

$$\mathsf{c_P}^{(\varphi^4)} = \mathcal{O}(\lambda\varphi_{\max}^4) = \mathcal{O}(\lambda 4^{\mathsf{n_q}})\,, \tag{134}$$

$$\mathsf{c_P}^{(\varphi_i\varphi_j)} = \mathcal{O}(\varphi_{\max}^2) = \mathcal{O}(2^{\mathsf{n_q}})\,. \tag{135}$$

As was the case with $\mathsf{N_P}$, the overall value of $\mathsf{c_P}$ is dominated by the $\hat{\varphi}^4$ term, and is given by

$$\mathsf{c_P} = \mathcal{O}(\lambda 4^{\mathsf{n_q}})\,. \tag{136}$$

These values for $\mathsf{N_P}$, $\mathsf{c_P}$ and $\mathsf{N_H}$ will be used in the following sections to determine the asymptotic gate complexity of the various time-evolution algorithms discussed in Sec. II E for geometrically site-local Hamiltonians.

B. Product formulas

In this section, we consider using a p^{th} order PF (introduced in Sec. II A) to time evolve the scalar field theory Hamiltonian (given by Eq. (121)) that has been digitized using the formalism presented in Section IV A 1.

Specifically, we construct concrete error bounds and asymptotic gate complexity estimates as a special case of the results obtained in Sec. III A for general geometrically site-local Hamiltonians. We use the result of Theorem 16 for the asymptotic bound on the elementary gate count χ (see Eq. (106)) and make the following substitutions based on the discussion provided in Section IV A 1:

$$\mathsf{N_H} = \mathcal{O}(\mathsf{N_\Lambda}), \tag{137}$$

$$\mathsf{N_P} = \mathcal{O}({\mathsf{n_q}}^4), \tag{138}$$

$$\mathsf{c_P} = \mathcal{O}(\lambda 4^{\mathsf{n_q}}). \tag{139}$$

These follow from Eq. (13), Eq. (131), and (136) respectively. Putting this all together, the asymptotic gate complexity is thus given by

$$\chi = \mathcal{O}\left(\mathsf{n_q}^{4\left(2+\frac{1}{p}\right)} \frac{\left(4^{\mathsf{n_q}}\mathsf{N_\Lambda}\lambda t\right)^{1+\frac{1}{p}}}{\varepsilon^{\frac{1}{p}}}\right). \tag{140}$$

C. QSP

Obtaining gate counts for the case of pure QSP requires two logical steps. The first is to determine the number of calls to the local block encoding, and the second is to estimate the complexity of implementing this block encoding. By Theorem 9, the query complexity for simulating with evolution time t to exponentiation error ε is given by

$$\mathcal{O}(\alpha t + \log(1/\varepsilon)), \tag{141}$$

where α is the scale factor of the BE used.

We now consider three approaches to implementing the local block encoding. The first approach is based on the fully general LCU procedure, and does not take into account any features of the model. The second approach is a modification of the former which takes advantage from splitting the Hamiltonian into the field and momentum parts, in analogy with how it was done in the product-formula-based approach. The third approach uses the QETU algorithm and implements the block encoding of the local Hamiltonian using the time evolution input model and then adding the local pieces using LCU. In this section, we consider only asymptotic gate complexities; detailed gate count comparisons of these techniques will be given in Sec. IV E.

1. Block encoding via LCU

In this section, we determine the cost of implementing time-evolution via QSP where the BE is implementing using a fully general LCU procedure; we first construct the digitized matrix $\hat{H}$ and then decompose it into Pauli strings. The most naive option would be to decompose the $\hat{\pi}_i^2$ operator into $\mathcal{O}(4^{\mathsf{n_q}})$ Pauli strings. The value of $\mathsf{c_P}$ in this case is the same as in Eq. (136). Lastly, we have $\mathsf{N_H} = \mathcal{O}(\mathsf{N_\Lambda})$. Plugging these results into Theorem 18 leads to an elementary gate complexity of

$$\chi = \mathcal{O}\Big[\mathsf{N_\Lambda} 3^{\mathsf{n_q}} \log\left(\mathsf{N_\Lambda} 3^{\mathsf{n_q}}\right)\left(\mathsf{N_\Lambda} 3^{\mathsf{n_q}}(\lambda 4^{\mathsf{n_q}})t + \log(1/\varepsilon)\right)\Big]. \tag{142}$$

We see that the naive decomposition of the $\hat{\pi}_i^2$ operators into Pauli gates results in a poor scaling with $\mathsf{n_q}$.

2. Block encoding via LCU and FT

In order to take advantage of decomposition (127) within the LCU construction, one needs to slightly modify the PREPARE and SELECT oracles. To write $\hat{H}$ in the form required for LCU, we first write the momentum component of $\hat{H}$ in the momentum basis as a sum of M_π unitary operators

$$\hat{H}_\pi^{(p)} = \sum_{j=0}^{M_\pi} \beta_j^{(\pi^{(p)})} \hat{U}_j^{(\pi^{(p)})}. \tag{143}$$

Next, we write the full Hamiltonian as

$$\hat{H} = \sum_{i=0}^{M_\varphi - 1} \beta_i^{(\varphi)} \hat{U}_j^{(\varphi)} + \mathrm{FT}\left(\sum_{j=0}^{M_\pi - 1} \beta_j^{(\pi^{(p)})} \hat{U}_j^{(\pi^{(p)})}\right)\mathrm{FT}^\dagger, \tag{144}$$

where it is understood that the Fourier transform is performed locally at each site. The Hamiltonian is now in a form where we can describe the modified LCU procedure.

First, the PREPARE oracle is used to encode the real positive coefficients $\beta_i^{(\varphi)}$ and $\beta_j^{(\pi^{(p)})}$. The SELECT oracle we need is given by

$$\begin{aligned} \text{SELECT} &= (\mathbb{1}_a \otimes \mathrm{FT}) \\ &\otimes \left(\sum_{j=0}^{M_\pi - 1} |j\rangle_a \langle j|_a \otimes \hat{U}_j^{(\pi^{(p)})}\right)(\mathbb{1}_a \otimes \mathrm{FT}^\dagger) \\ &+ \sum_{i=0}^{M_\varphi - 1} |i + M_\pi\rangle_a \langle i + M_\pi|_a \otimes \hat{U}_i^{(\varphi)}. \end{aligned} \tag{145}$$

Constructing the circuit for U is achieved by applying the Fourier transform on the state register (again at each lattice site), implementing the controlled versions of each $\hat{U}_j^{(\pi^{(p)})}$, applying the inverse Fourier transform on the state register, and finally implementing the controlled versions of each $\hat{U}_i^{(\varphi)}$.

Note that the SELECT oracle prepared using this method is equivalent to the SELECT oracle prepared using the naive LCU procedure in Sec. IV C 1; the only difference is how it is implemented. This different implementation, however, results in a more favorable scaling for $\mathsf{N_P}$. This can be understood by noting that the $\mathsf{N_P}$ associated with the momentum Hamiltonian is reduced to $\mathsf{N_P}^{(\pi^{(p)})} = \mathcal{O}(\mathsf{n_q}^2)$, implying that the value of $\mathsf{N_P}$ is dominated by the $\hat{\varphi}^4$ term. Substituting $\mathsf{N_P} = \mathcal{O}(\mathsf{n_q}^4)$, $\mathsf{c_P} = \mathcal{O}(\lambda 4^{\mathsf{n_q}})$ and $\mathsf{N_H} = \mathcal{O}(\mathsf{N_\Lambda})$ into the result in Theorem 18 gives the gate complexity

$$\chi = \mathcal{O}\Big[\mathsf{N_\Lambda}\mathsf{n_q}^4 \log(\mathsf{N_\Lambda}\mathsf{n_q}^4)\left(\mathsf{N_\Lambda}\mathsf{n_q}^4(\lambda 4^{\mathsf{n_q}})t + \log(1/\varepsilon)\right)\Big], \tag{146}$$

which has a more favorable scaling with $\mathsf{n_q}$ than the naive LCU implementation in Sec. IV C 1.

3. Block encoding via QETU

In this section, we develop a novel application of the QETU algorithm. While it has been originally proposed as a way to eliminate the necessity of using the block encoding in the early-fault-tolerant quantum algorithms [30], below we show that, in fact, it can as well be used as a highly-efficient tool for constructing block encodings. The general strategy is to use QETU to prepare local BEs of individual terms in the Hamiltonian, and then add these terms using LCU. To do this, we first need to write the Hamiltonian in terms of functions of the operators $\hat{\pi}_i$ and $\hat{\varphi}_i$. Note that, in general, the choice of functions we decompose the Hamiltonian into is not unique. One can choose a different function as long as one modifies the operator used as a building block accordingly. To understand the general arguments for the most cost effective choices, we first work through a simple example and then generalize the arguments.

Consider using QETU to block-encode the term $\hat{\varphi}_i^2$. One choice would be to choose $\mathsf{f}(x) = x^2$ and use $\mathrm{e}^{-i\tau\hat{\varphi}_i}$ as a building block. Another equally valid choice would be to set $\mathsf{f}(x) = x$ and use the somewhat more expensive operator $\mathrm{e}^{-i\tau\hat{\varphi}_i^2}$ as a building block. Comparing the cost of the building blocks, as previously discussed, the circuit for $\mathrm{e}^{-i\tau\hat{\varphi}_i}$ requires $\mathsf{n_q}$ rotation gates and zero CNOT gates, while the circuit for $\mathrm{e}^{-i\tau\hat{\varphi}_i^2}$ requires $\mathcal{O}(\mathsf{n_q}^2)$ rotation *and* CNOT gates. We now compare the convergence properties of Chebyshev approximations to the different choices of functions. Setting $\tau = \pi/c_2$, the first and second choices lead to $\mathsf{F}(x) \sim \arcsin(x)^2$ and $\mathsf{F}(x) \sim \arcsin(x)$, respectively. Both choices have a discontinuous first derivative at $x = \pm 1$, and therefore we expect the Chebyshev approximation in both cases to converge with the same asymptotic polynomial degree. This implies that using the (first) choice with the cheaper building block will require less overall gates for the same desired precision.

From this example we learned that, if the function we want to block-encode is a polynomial (as is the case with H_{quartic}), it is more cost effective to choose the function $\mathsf{f}(x)$ that results in the cheapest building block possible. Using this guiding principle, the form of the Hamiltonian we choose is

$$\hat{H}_{\text{quartic}} = \sum_{i=1}^{\mathsf{N}_\Lambda} \left(\mathrm{FT}_i \, \mathsf{f}(\hat{\pi}_i^{(p)}, 0) \mathrm{FT}_i^\dagger + \mathsf{f}(\hat{\varphi}_i, \lambda) \right) + \sum_{\langle ij \rangle} \mathsf{f}(\hat{\varphi}_j - \hat{\varphi}_i, 0) \,, \tag{147}$$

where we have used the Fourier transform to allow us to work with the diagonal operators $\hat{\pi}_i^{(p)}$, and

$$\mathsf{f}(x, \lambda) = \frac{1}{2} x^2 + \frac{\lambda}{4!} x^4 \,. \tag{148}$$

The strategy is to use QETU to implement the matrix functions $\mathsf{f}(\hat{\pi}_i^{(p)}, 0)$, $\mathsf{f}(\hat{\varphi}_i, \lambda)$ and $\mathsf{f}(\hat{\varphi}_j - \hat{\varphi}_i, 0)$ exactly. We now consider the cost of each term separately.

To implement $\mathsf{f}(\hat{\pi}_i^{(p)}, 0)$, we will perform repeated calls to controlled versions of $\mathrm{e}^{-i\tau\hat{\pi}_i^{(p)}}$. The operator $\mathrm{e}^{-i\tau\hat{\pi}_i^{(p)}}$ can be implemented using only $\mathsf{n_q}$ rotation gates. The controlled implementation therefore requires $\mathcal{O}(\mathsf{n_q})$ rotation gates and $\mathcal{O}(\mathsf{n_q})$ CNOT gates. Because $\hat{\pi}_i^{(p)}$ has $\mathcal{O}(2^{\mathsf{n_q}})$ distinct eigenvalues, one can exactly implement $\mathsf{F}(\hat{\pi}_i^{(p)}) \sim \arcsin(\hat{\pi}_i^{(p)})^2$ using a Chebyshev approximation with $\mathcal{O}(2^{\mathsf{n_q}})$ polynomials. The cost of the Fourier transform is $\mathcal{O}(\mathsf{n_q}^2)$ which is sub-leading, leading to a gate complexity of $\mathcal{O}(\mathsf{n_q} 2^{\mathsf{n_q}})$.

Similar arguments can be used for implementing the $\mathsf{f}(\hat{\varphi}_i, \lambda)$ terms. The controlled call to the building block $\mathrm{e}^{-i\tau\hat{\varphi}_i}$ requires $\mathcal{O}(\mathsf{n_q})$ rotation and CNOT gates. Implementing the function $\mathsf{F}(\hat{\varphi}_i) \sim m^2 \arcsin(\hat{\varphi}_i)^2 + \lambda \arcsin(\hat{\varphi}_i)^4$ exactly requires using $\mathcal{O}(2^{\mathsf{n_q}})$ Chebyshev polynomials. Taken together, the total cost of implementing a single $\mathsf{f}(\hat{\varphi}_i, \lambda)$ term is $\chi_\varphi = \mathcal{O}(\mathsf{n_q} 2^{\mathsf{n_q}})$.

The final function we need to implement is $\mathsf{f}(\hat{\varphi}_j - \hat{\varphi}_i, 0)$. The building block in this case is $\mathrm{e}^{-i\tau(\hat{\varphi}_j - \hat{\varphi}_i)}$, which, owing to commutativity of $\hat{\varphi}_i$ and $\hat{\varphi}_j$ acting on different Hilbert spaces, factorizes to $\mathrm{e}^{-i\tau\hat{\varphi}_j} \otimes \mathrm{e}^{i\tau\hat{\varphi}_i}$; the controlled version of this operator therefore requires $2\mathsf{n_q}$ CNOT and rotation gates. Using $\mathcal{O}(2^{\mathsf{n_q}})$ Chebyshev polynomials to implement $\mathsf{F}(\hat{\varphi}_j - \hat{\varphi}_i) \sim \arcsin(\hat{\varphi}_j - \hat{\varphi}_i)^2$ exactly for a single term therefore has a gate complexity $\mathcal{O}(\mathsf{n_q} 2^{\mathsf{n_q}})$.

The next step is to add each of the $\mathcal{O}(\mathsf{N}_\Lambda)$ local terms together using LCU. To determine the total cost of LCU, we use the fact that, if implementing the non-controlled operator U requires χ_U gates, the multi-qubit controlled operation on k qubits requires $\mathcal{O}(\chi_U \, k)$ gates [32, 60]. Identifying $k = \mathcal{O}(\log \mathsf{N}_\Lambda)$, we find that the gate cost of implementing the BE of any local term is $\mathcal{O}(\mathsf{n_q} 2^{\mathsf{n_q}} \log \mathsf{N}_\Lambda)$. The total gate complexity of preparing a BE of $\hat{H}_{\text{quartic}}$ is therefore $\mathcal{O}(\mathsf{n_q} 2^{\mathsf{n_q}} \mathsf{N}_\Lambda \log \mathsf{N}_\Lambda)$.

The final piece is to determine the scale factor α when using QETU to prepare the block encoding for $\hat{H}_{\text{quartic}}$. The BE of each function in the Hamiltonian is prepared such that $|\mathsf{F}(x)| \leq 1, \forall x \in [-1, 1]$. In practice, to minimize the scale factor, one would choose $\max_x(|\mathsf{F}(x)|) = 1$, implying that the scale factor can be found as $\alpha = \max_x(|\mathsf{F}(x)|), \forall x \in [-1, 1]$. For our case, the function $|\mathsf{F}(x)|$ is maximized for

$x = \pm 1$. Setting $x = 1$, we have $\mathsf{F}(x = 1) = \mathsf{f}(c_2/c_1)$. The ratio c_2/c_1 depends on the minimum and maximum eigenvalues of the operator considered. Using the fact that our choice of digitization lead to $\pi_{\min} = -\pi_{\max}$ and $\varphi_{\min} = -\varphi_{\max}$, for $\hat{a}_j = \{\hat{\pi}_j^{(p)}, \hat{\varphi}_j\}$ this ratio is given by

$$\frac{c_2}{c_1} = \frac{\eta(a_{\max} - a_{\min})}{\pi - 2\eta} - a_{\min} = \mathcal{O}(a_{\max}) \,. \quad (149)$$

Using the fact that our choice of digitization leads to $\pi_{\max} = \mathcal{O}(2^{\mathsf{n_q}/2})$ and $\varphi_{\max} = \mathcal{O}(2^{\mathsf{n_q}/2})$, the dominant local contribution to the scale factor is nothing other than the maximum coefficient $\mathsf{c_P}$ of any Pauli-string, given by $\mathsf{c_P} = \mathcal{O}(\lambda 4^{\mathsf{n_q}})$. The overall scale factor from adding the local terms at each lattice site is then

$$\alpha = \mathcal{O}(\lambda 4^{\mathsf{n_q}} \mathsf{N}_\Lambda) \,. \quad (150)$$

Combining this result for the scale factor with the cost of using LCU to block-encode the Hamiltonian, the total cost of using QSP to time-evolve for a time t to precision ε is

$$\chi = \mathcal{O}\Big[\mathsf{n_q} 2^{\mathsf{n_q}} \mathsf{N}_\Lambda \log \mathsf{N}_\Lambda \left((\lambda 4^{\mathsf{n_q}})\mathsf{N}_\Lambda t + \log(1/\varepsilon)\right)\Big] \,. \quad (151)$$

We conclude by pointing out a technical detail. To optimize the value of α, one needs to choose a different value of α for each $\mathsf{f}(x, \lambda)$ appearing in the Hamiltonian. Care will have to be taken when choosing what coefficients are used when adding the local terms using LCU to ensure the relative magnitudes of each operator is maintained.

D. HHKL

In order to apply the HHKL results formulated in our conventions in Theorem 24 and Theorem 25, note that we must scale down the Hamiltonian (121) by the appropriate factor that brings the local terms to at most unit spectral norm, and simultaneously rescale evolution time up by the same factor. This factor is precisely the maximum spectral norm of any local term $\tilde{H}_J$,

$$\begin{aligned} &\max_{J\in S} \|\tilde{H}_J\| \\ &= \left\| \frac{1}{2}\hat{\pi}_i^2 + \frac{1}{2}m^2\hat{\varphi}_i^2 + \frac{\lambda}{4!}\hat{\varphi}_i^4 + \sum_{j\in\langle ij\rangle} \frac{(\hat{\varphi}_j - \hat{\varphi}_i)^2}{2} \right\| \\ &= \mathcal{O}(\mathsf{N_P}\mathsf{c_P}) = \mathcal{O}({\mathsf{n_q}}^4(\lambda 4^{\mathsf{n_q}})) \,, \end{aligned} \quad (152)$$

where we have used $\mathsf{N_P} = \mathcal{O}({\mathsf{n_q}}^4)$ and $\mathsf{c_P} = \mathcal{O}(\lambda 4^{\mathsf{n_q}})$, and where any lattice site with index i in the interior of the lattice (or on the boundary if there are no sites in the interior) can be chosen to compute the spectral norm, and the sum runs over all lattice sites j neighboring i. We therefore make the rescalings

$$\tilde{H} = \frac{H}{\max_{J\in S} \|H_J\|} \quad (153)$$

$$\tilde{t} = t \max_{J\in S} \|H_J\| = \mathcal{O}(4^{\mathsf{n_q}} {\mathsf{n_q}}^4 \lambda t) \,. \quad (154)$$

For HHKL built out of local Trotter operations, Theorem 24 implies a gate complexity

$$\chi = \mathcal{O}\Big[{\mathsf{n_q}}^4 (\mathsf{N}_\Lambda {\mathsf{n_q}}^4 (\lambda 4^{\mathsf{n_q}})t)^{1+\frac{1}{p}} \varepsilon^{-\frac{1}{p}}\Big] \,. \quad (155)$$

where we substituted $\mathsf{c_P} = \mathcal{O}(\lambda 4^{\mathsf{n_q}})$ and $\mathsf{N_P} = \mathcal{O}({\mathsf{n_q}}^4)$.

Similarly, for HHKL built out of local QSP operations, Theorem 25 then implies a gate complexity

$$\begin{aligned} \chi = \mathcal{O}\Big[&({\mathsf{n_q}}^4)^2 \mathsf{N}_\Lambda (\lambda 4^{\mathsf{n_q}}) t \log^{\mathsf{d}} \left(\mathsf{N}_\Lambda t/\varepsilon\right) \\ &\times \log\left({\mathsf{n_q}}^4 \log\left(\mathsf{N}_\Lambda t/\varepsilon\right)\right)\Big] . \end{aligned} \quad (156)$$

To conclude our discussion on HHKL scalings, we again stress an important point. As we have previously remarked, while the purely asymptotic scaling of the Trotter-based HHKL gate count is worse than that for QSP-based HHKL, the difference is not striking when the Trotter order p is taken to be large. This allows for the possibility of lower constant prefactors due to the smaller overhead involved in implementing Trotter operations compared to QSP operations, and may even be a prudent choice for a more practical implementation on near-term devices, if the exact gate counts follow suit before asymptotics take over.

E. Numerical results.

In the previous section we worked out the asymptotic gate count scaling for several time-evolution algorithms. While these expressions are helpful for identifying which methods have the best scaling in a particular parameter, the practical question of the size of the prefactors requires a dedicated numerical study, which we perform in this section. In particular, we first compare the cost of the three BE methods described in the previous section. From there, we turn to time evolution and compare the cost of using QSP combined with the optimal BE method to that of a 2nd order PF, focusing on the scaling with time t and error ε.

We choose to focus on a single site Hamiltonian given by

$$\hat{H} = \frac{1}{2}\hat{\pi}^2 + \frac{1}{2}\hat{\varphi}^2 + \frac{\lambda}{4!}\hat{\varphi}^4 \,, \quad (157)$$

where we set $\lambda = 32$ (similarly to [11]) as an instance of the strongly coupled regime where perturbation theory breaks down. While this will not provide an explicit scaling with the number of lattice sites, analyzing the single site case in detail will provide intuition for what values of t and ε QSP outperforms PF methods for $\mathsf{N}_\Lambda > 1$.

The top and middle plots in Fig. 8 show the CNOT gate count and rotation gate count, respectively, for three different BE methods as a function of $\mathsf{n_q}$. The blue points show the gate counts using the LCU method where one naively decomposes the full digitized Hamiltonian into Pauli strings as described in Sec. IV C 1. As expected, this method scales least favorably with $\mathsf{n_q}$ and requires the largest number of ancillary qubits, as seen in the bottom plot of Fig. 8. As previously discussed in Sec. IV C 2, this poor gate scaling with $\mathsf{n_q}$ can be improved by utilizing the Fourier Transform to implement the momentum component of the Hamiltonian. This improved scaling can be seen by looking at the orange squares in the top and middle plots in Fig. 8. This method also requires less ancillary qubits, as shown in the bottom plot of Fig. 8. The final method we compare implements the BE using QETU as described in Sec. IV C 3. Looking at Fig. 8, we see that, while the gate cost of QETU (given in Eq. (151)) is asymptotically worse than LCU combined with the Fourier transform (given in Eq. (146)), the actual gate cost of using QETU is similar to the improved LCU method, and becomes cheaper for $\mathsf{n_q} \sim 10$. One advantage of the QETU method is that the number of ancillary qubits is independent of $\mathsf{n_q}$. Therefore, QETU is preferable when aiming to minimize the number of qubits.

Now that we have identified the optimal method for preparing BEs, we turn to the cost of performing time evolution. The first method we implement is a 2nd order PF. The second uses QSP, where the BE is prepared using the optimal BE method. Figure 9 shows the CNOT gate count for both methods as a function of evolution time t and error ε for $\mathsf{n_q} = 3$. Due to QSP's large overall prefactor from implementing the BE, using the 2nd order PF requires less gates for errors $\varepsilon \gtrsim 10^{-8}$. For errors $\varepsilon \lesssim 10^{-8}$, QSP wins due to its exponentially better scaling with respect to ε. In Sec. V we discuss the implications of these results for multi-site systems.

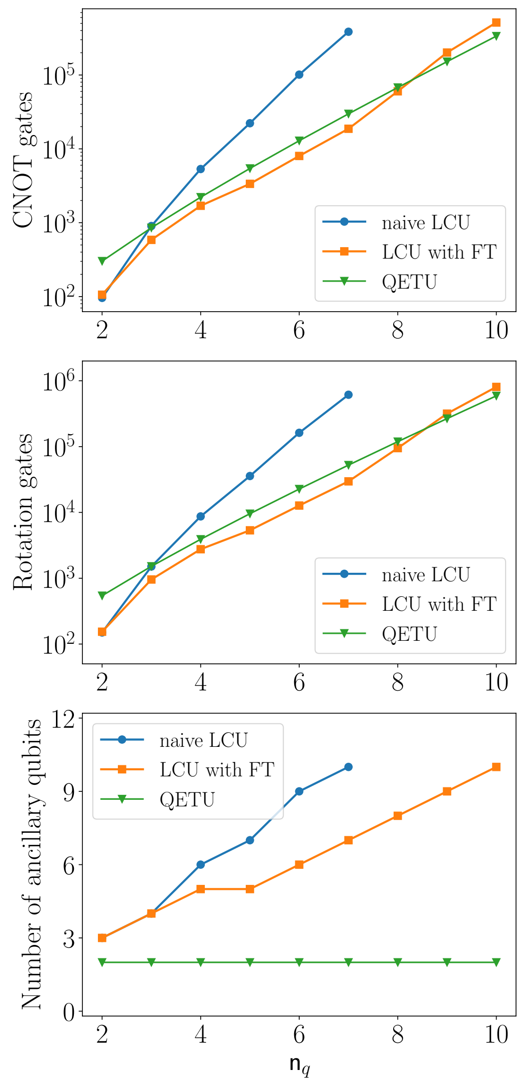

Figure 8. The top, middle, and bottom plots show the CNOT gate count, rotation gate count, and number of ancillary qubits needed to prepare a BE of the single site Hamiltonian in Eq. 157 as a function of $\mathsf{n_q}$. Different colored/shaped points correspond to different methods for preparing the BE. Blue circles correspond to using the naive LCU method described in Sec. IV C 1. Orange squares correspond to using LCU combined with the Fourier Transform as described in Sec. IV C 2. Green triangles correspond to using QETU as described in Sec. IV C 3. While the QETU method has a worse asymptotic scaling with $\mathsf{n_q}$ (see Eq. (151)) compared to the LCU method the Fourier transform (see Eq. (146)), the top and middle plots demonstrate that the two methods have a similar gate cost for $\mathsf{n_q} \sim 3 - 9$, and becomes cheaper for $\mathsf{n_q} = 9$. The bottom plot shows that QETU requires a constant number of qubits, while the other two methods require more qubits as $\mathsf{n_q}$ is increased.

V. DISCUSSION

In this section we discuss how results of Sec. III provide guidance for choosing a simulation algorithm for the particular physical model and then examine the results of Sec. IV.

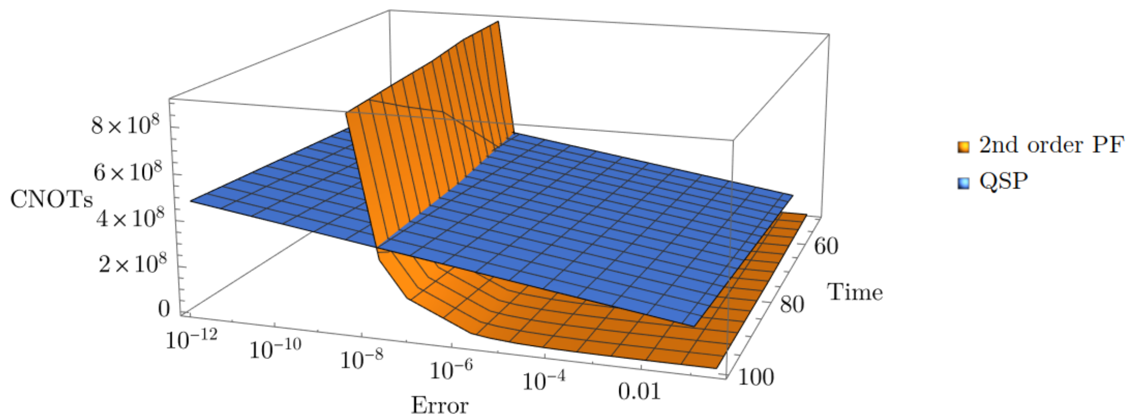

Figure 9. CNOT gate count for implementing the time evolution operator for the single site Hamiltonian in Eq. (121) with $\mathsf{n_q} = 3$. Results are shown as a function of time t and error ε. The orange and blue colored surfaces show results using a 2nd order PF and QSP, respectively. The BE used in the QSP calculation was implemented using the method in Sec. IV C 2. The PF requires less gates for errors $\varepsilon \gtrsim 10^{-8}$. For error tolerances $\varepsilon \lesssim 10^{-8}$, QSP wins due to its exponentially better scaling with ε.

A. The choice of simulation algorithm

The major parameters of interest defining the asymptotic complexities of time evolution algorithms are the evolution time t, the error of the time-evolved state ε, as well as some measure of Hamiltonian size/complexity. For lattice systems, this can be the number of terms in the Hamiltonian $\mathsf{N_H}$. For a particular theory, $\mathsf{N_H}$ can also be expressed in terms of lattice size $\mathsf{N_\Lambda}$. The dependence of $\mathsf{N_H}$ on $\mathsf{N_\Lambda}$ is linear for geometrically-site-local Hamiltonians and is, more generally, polynomial. For algorithms based on PFs, one additionally needs to consider a parameter $\mathsf{N_{ind}}$ related to the induced norm of the Hamiltonian. The asymptotic dependence on individual parameters for algorithms discussed in Secs. II and III is summarized in Table V.

The parameter for which the difference in asymptotic dependence is most striking for PF- and QSP-based algorithms is the error ε. Nevertheless, using algorithms with $\log(1/\varepsilon)$ dependence may not necessarily be an optimal choice for several reasons. First, their asymptotic cost comes with large constant prefactors stemming from the implementation of the BE subroutine. While progress is being made in this direction, the value of ε at which using such techniques clearly becomes advantageous is $\varepsilon \sim 10^{-8}$, which is much smaller than uncertainties coming from other sources (e.g., from digitizing a theory with bosonic degrees of freedom, finite lattice spacing and volume effects, to name just a few). Second, as discussed below, in some scenarios PF-based algorithms have better dependence on problem size than those based on QSP. Third, and least importantly (in the fault-tolerant regime), PF based algorithms do not require the usage of ancillary qubits, while QSP-based algorithms typically require a logarithmic (in problem parameters) number of those.

In terms of the asymptotic dependence on problem size, a clear winner is the HHKL algorithm, assuming that for implementing the time evolution of local blocks, an algorithm with $\log(1/\varepsilon)$ scaling is chosen, such as QSP. Note, however, that for higher-order PFs [27] the improvement reached by the HHKL algorithm in terms of problem size may not be particularly pronounced, especially, unless a very high precision is required, as discussed above.

For non-geometrically-local Hamiltonians, the situation is largely determined by the Hamiltonian structure defining the dependence of $\mathsf{N_{ind}}$ on $\mathsf{N_\Lambda}$. In particular, in the second-quantized formulation, this dependence will be defined by the choice of single-particle basis states (plane waves [9, 33], wavelets [65], harmonic oscillator eigenstates [10], etc.). Importantly, whether the Hamiltonian is geometrically-local or not, one can imagine scenarios in which, at a fixed value of ε, switching from PF to QSP would make sense as one increases the problem size. However, given the sharp difference in the dependence on ε for these approaches, such scenarios are not highly probable.

Lastly, we note that the dependence on t is likely to not be a crucial parameter in choosing the simulation algorithm. Nevertheless, a situation in which considering longer times can motivate one to switch from PF to QSP is possible as well.

In addition to factors considered in this work, other considerations should also be taken into ac-

	ε	t	$\mathsf{N_H}$
Non-geometrically-local			
a) PF	$\varepsilon^{-\frac{1}{p}}$	$t^{1+\frac{1}{p}}$	$\boldsymbol{\mathsf{N_H}^{1+\frac{1}{p}}\mathsf{N_{ind}}}$
b) QSP+PF	$\varepsilon^{-\frac{1}{p}}\log(1/\varepsilon)$	$t^{1+\frac{1}{p}}$	$\mathsf{N_H}^{1+\frac{1}{p}}\mathsf{N_{ind}} \times \log(\mathsf{N_H}\mathsf{N_{ind}})$
c) QSP	$\boldsymbol{\log(1/\varepsilon)}$	$\boldsymbol{t}$	$\boldsymbol{\mathsf{N_H}^2\log(\mathsf{N_H})}$
Geometrically-local	ε	t	$\mathsf{N_\Lambda}$
d) PF	$\varepsilon^{-\frac{1}{p}}$	$t^{1+\frac{1}{p}}$	$\mathsf{N_\Lambda}^{1+\frac{1}{p}}$
e) PF+HHKL	$\varepsilon^{-\frac{1}{p}}$	$t^{1+\frac{1}{p}}$	$\mathsf{N_\Lambda}^{1+\frac{1}{p}}$
f) QSP+PF	$\varepsilon^{-\frac{1}{p}}\log(1/\varepsilon)$	$t^{1+\frac{1}{p}}$	$\mathsf{N_\Lambda}^{1+\frac{1}{p}}\log(\mathsf{N_\Lambda})$
g) QSP	$\boldsymbol{\log(1/\varepsilon)}$	$\boldsymbol{t}$	$\mathsf{N_\Lambda}^2$
h) QSP+HHKL	$\boldsymbol{\log(1/\varepsilon)}$	$\boldsymbol{t}$	$\boldsymbol{\mathsf{N_\Lambda}[\log(\mathsf{N_\Lambda})]^{\mathsf{d}} \times \log\log(\mathsf{N_\Lambda})}$

Table V. Asymptotic dependence ($\mathcal{O}$ omitted) on major problem parameters for algorithms in Tables III and IV. Boldface indicates best asymptotic scaling among applicable methods. While $\mathsf{N_{ind}}$ is constant for geometrically-local theories, it typically scales polynomially with $\mathsf{N_\Lambda}$ otherwise. For most non-geometrically-local theories, the order p can be chosen large enough so that PFs demonstrate better scaling with $\mathsf{N_\Lambda}$ than QSP.

count. Most notably, the compatibility of methods based on BE with general sparse Hamiltonians and modern simulation techniques [66–68] and the potential for applying the PF-based methods on early-fault-tolerant quantum computers [30, 69].

B. Novel approaches to bosonic block encodings

Construction of efficient block encodings (BEs) is critical for improving the efficiency of QSP-based algorithms. BEs considered in Secs. IV C 2 and IV C 3 provide examples of how the additional knowledge of system's structure can typically be utilized for improving the algorithm efficiency [32–34, 47]. In Refs. [11, 19] it was shown how digitizing a bosonic degree of freedom in the eigenbases of position/momentum operator is advantageous from the perspective of using PF algorithms. There, the key factors are a) an economical qubit representation of arbitrary powers of position/momentum operators in their respective eigenbases and b) the efficiency of switching between the position and momentum bases with the aid of Fourier Transform implemented on the quantum computer. In Sec. IV C 2 we showed how this approach can be equally well applied when constructing a BE with LCU.

In Sec. IV C 1 we continued the investigation of the capabilities of the QETU algorithm which we started in Ref. [42]. We showed that, while being originally developed for avoiding the usage of BEs in nearly-optimal simulation algorithms, the QETU technique can also be used as a highly-efficient tool for constructing them. Most generally, the QETU technique opens the door to combining methods based on PF and QSP. In particular, an interesting direction for further exploration is the possibility of constructing BEs with circuit depth (i.e., the number of layers in the circuit) sub-linear in $\mathsf{N_\Lambda}$ for geometrically-local systems. While constructing a BE with gate cost sub-linear in the lattice size does not seem realistic, we do not see fundamental obstacles for parallelizing operations acting on different qubits.

VI. CONCLUSION

In this work we studied various approaches to simulating time evolution in application to Hamiltonian Lattice Field Theories (HLFTs). We started off by providing a review of existing techniques based on Product Formula (PF) splitting [28], Quantum Signal Processing (QSP) [43] and Qubitization [44], Linear Combination of Unitaries (LCU) [29], Quantum Eigenvalue Transformation of Unitary Matrices (QETU) [30], as well as the HHKL algorithm [45]. Following that, we derived asymptotic costs of these methods in terms of parameters describing site-local and geometrically-site-local Hamiltonians arising in HLFT, see Tables III and IV. While in this work we chose to contrast the most accessible and widely used algorithms based on PF with the methods having the best asymptotic scaling (QSP, HHKL), we note that there exist intermediate approaches. Most notably, this includes the direct usage of Taylor series and LCU without QSP [70].

Next, we focused on a particular type of HLFT, the quartic scalar field theory defined on a hypercubic lattice. Our specific choice was guided by the fact that all the fundamental interactions are mediated by bosons, and from the computational perspective the scalar field theory is largely reminiscent of lattice gauge theories. Besides this, an extensive volume of literature exists focusing on simulations of fermionic systems [31, 32, 47, 71–77]. Developing simulation algorithms for systems combining particles of both statistics is an exciting direction which was pursued in Refs. [61, 62, 78] where authors assumed the usage of PF-based methods, and is currently investigated in the context of nearly-optimal techniques [35].

For the scalar field theory, we worked out the query complexities of various simulation methods and provided a detailed description of various approaches to constructing BEs for bosonic degrees of freedom. In particular, we employed a generic LCU procedure, an LCU procedure utilizing the Fourier Transform circuit for switching between the position and momentum bases, as well as a novel approach based on the usage of QETU algorithm, see Fig. 8 for comparison.

Another important distinction between PF and QSP methods is the ease of quoting accurate error bounds for the final result. Starting with QSP methods, all that is needed to place an upper bound on the error is the scale factor α, the time t, and the degree of the polynomial approximation. While the error determined in this way is only an upper bound, because QSP methods have optimal scaling $\log(1/\varepsilon)$ in the error, the cost of overestimating the error is low compared to the contribution stemming from the αt term in Eq. (63).

For PF methods on the other hand, while rigorous error bounds also exist, they are known to generally significantly overestimate the actual error [28]. Choosing the value of the Trotter number r based on these loose error bounds would therefore result in significant extra computational costs due to the sub-optimal $(1/\varepsilon)^p$ scaling of PF methods. Tightening error bounds in this case implies either performing laborious problem-specific commutator calculations [28, 78] or performing numerical simulations at several values of the Trotter number in order to extrapolate the results. As shown in Ref. [79], since using PFs to approximate the time evolution operator is equivalent to introducing a temporal lattice with spacing a_t, such an extrapolation would necessitate a renormalization procedure with a costly scale setting procedure at each value of a_t.[16]

ACKNOWLEDGEMENTS

The authors are grateful to Jeongwan Haah, Lin Lin, and Ivan Mauricio Burbano Aldana for discussions and comments. SH acknowledges support from the Berkeley Center for Theoretical Physics and the National Energy Research Scientific Computing Center (NERSC), a U.S. Department of Energy Office of Science User Facility located at Lawrence Berkeley National Laboratory, operated under Contract No. DE-AC02- 05CH11231. CWB and MK were supported by the DOE, Office of Science under contract DE-AC02-05CH11231, partially through Quantum Information Science Enabled Discovery (QuantISED) for High Energy Physics (KA2401032). This material is based upon work supported by the U.S. Department of Energy, Office of Science, Office of Advanced Scientific Computing Research, Department of Energy Computational Science Graduate Fellowship under Award Number DE-SC0020347.

[1] Z. Davoudi *et al.*, in *Snowmass 2021* (2022) arXiv:2209.10758 [hep-lat].
[2] C. Morningstar, in *21st Annual Hampton University Graduate Studies Program (HUGS 2006)* (2007) arXiv:hep-lat/0702020.
[3] E. Y. Loh, J. E. Gubernatis, R. T. Scalettar, S. R. White, D. J. Scalapino, and R. L. Sugar, Phys. Rev. B **41**, 9301 (1990).
[4] G. Pan and Z. Y. Meng, (2022), 10.1016/B978-0-323-90800-9.00095-0, arXiv:2204.08777 [cond-mat.str-el].
[5] J. B. Kogut and L. Susskind, Phys. Rev. D **11**, 395 (1975).
[6] S. D. Drell, H. R. Quinn, B. Svetitsky, and M. Weinstein, Physical Review D **19**, 619 (1979).
[7] W. A. Bardeen and R. B. Pearson, Physical Review D **14**, 547 (1976).
[8] W. A. Bardeen, R. B. Pearson, and E. Rabinovici, Phys. Rev. D **21**, 1037 (1980).
[9] J. Liu, Z. Li, H. Zheng, X. Yuan, and J. Sun, Mach. Learn. Sci. Tech. **3**, 045030 (2022), arXiv:2109.05547 [quant-ph].
[10] J. P. Vary, H. Honkanen, J. Li, P. Maris, S. J. Brodsky, A. Harindranath, G. F. de Teramond, P. Sternberg, E. G. Ng, and C. Yang, Phys. Rev. C **81**, 035205 (2010), arXiv:0905.1411 [nucl-th].
[11] N. Klco and M. J. Savage, Phys. Rev. A **99**, 052335 (2019), arXiv:1808.10378 [quant-ph].
[12] H. C. Pauli and S. J. Brodsky, Phys. Rev. D **32**, 1993 (1985).
[13] H.-C. Pauli and S. J. Brodsky, Physical Review D **32**, 2001 (1985).
[14] S. J. Brodsky, H.-C. Pauli, and S. S. Pinsky, Phys. Rept. **301**, 299 (1998), arXiv:hep-ph/9705477.
[15] S. P. Jordan, H. Krovi, K. S. M. Lee, and J. Preskill, Quantum **2**, 44 (2018), arXiv:1703.00454 [quant-ph].
[16] S. P. Jordan, K. S. M. Lee, and J. Preskill, Science **336**, 1130 (2012), arXiv:1111.3633 [quant-ph].
[17] R. P. Feynman, Int. J. Theor. Phys. **21**, 467 (1982).
[18] C. W. Bauer *et al.*, PRX Quantum **4**, 027001 (2023), arXiv:2204.03381 [quant-ph].

[16] As was also shown in Ref. [79], to avoid a double extrapolation $a \to 0$ and $a_t \to 0$, one should work at fixed anisotropy $\xi \equiv a/a_t$ and take the limit $a \to 0$.

[19] S. P. Jordan, K. S. M. Lee, and J. Preskill, Quant. Inf. Comput. **14**, 1014 (2014), arXiv:1112.4833 [hep-th].

[20] S. Lloyd, Science **273**, 1073 (1996).

[21] C. Zalka, Proceedings of the Royal Society of London. Series A: Mathematical, Physical and Engineering Sciences **454**, 313 (1998).

[22] S. Wiesner, (1996), arXiv:quant-ph/9603028.

[23] J. E. Cohen, S. Friedland, T. Kato, and F. P. Kelly, Linear Algebra and its Applications **45**, 55 (1982).

[24] M. Suzuki, Communications in Mathematical Physics **51**, 183 (1976).

[25] N. Hatano and M. Suzuki, Lect. Notes Phys. **679**, 37 (2005), arXiv:math-ph/0506007.

[26] M. Suzuki, J. Math. Phys. **32**, 400 (1991).

[27] A. M. Childs and Y. Su, Physical review letters **123**, 050503 (2019).

[28] A. M. Childs, Y. Su, M. C. Tran, N. Wiebe, and S. Zhu, Phys. Rev. X **11**, 011020 (2021), arXiv:1912.08854 [quant-ph].

[29] A. M. Childs and N. Wiebe, Quant. Inf. Comput. **12**, 0901 (2012), arXiv:1202.5822 [quant-ph].

[30] Y. Dong, L. Lin, and Y. Tong, PRX Quantum **3**, 040305 (2022), arXiv:2204.05955 [quant-ph].

[31] B. Toloui and P. J. Love, (2013), arXiv:1312.2579 [quant-ph].

[32] R. Babbush, C. Gidney, D. W. Berry, N. Wiebe, J. McClean, A. Paler, A. Fowler, and H. Neven, Phys. Rev. X **8**, 041015 (2018).

[33] M. Kreshchuk, W. M. Kirby, G. Goldstein, H. Beauchemin, and P. J. Love, Phys. Rev. A **105**, 032418 (2022), arXiv:2002.04016 [quant-ph].

[34] W. M. Kirby, S. Hadi, M. Kreshchuk, and P. J. Love, Phys. Rev. A **104**, 042607 (2021), arXiv:2105.10941 [quant-ph].

[35] M. L. Rhodes, M. Kreshchuk, and S. Pathak, "Efficient constructions of block-encoding oracles for simulating lattice gauge theory," In preparation.

[36] J. F. Haase, L. Dellantonio, A. Celi, D. Paulson, A. Kan, K. Jansen, and C. A. Muschik, Quantum **5**, 393 (2021), arXiv:2006.14160 [quant-ph].

[37] Y. Ji, H. Lamm, and S. Zhu (NuQS), Phys. Rev. D **102**, 114513 (2020), arXiv:2005.14221 [hep-lat].

[38] C. W. Bauer and D. M. Grabowska, Phys. Rev. D **107**, L031503 (2023), arXiv:2111.08015 [hep-ph].

[39] C. W. Bauer, I. D'Andrea, M. Freytsis, and D. M. Grabowska, (2023), arXiv:2307.11829 [hep-ph].

[40] D. M. Grabowska, C. Kane, B. Nachman, and C. W. Bauer, (2022), arXiv:2208.03333 [quant-ph].

[41] C. Kane, D. M. Grabowska, B. Nachman, and C. W. Bauer, (2022), arXiv:2211.10497 [quant-ph].

[42] C. F. Kane, N. Gomes, and M. Kreshchuk, (2023), arXiv:2310.13757 [quant-ph].

[43] G. H. Low and I. L. Chuang, Phys. Rev. Lett. **118**, 010501 (2017), arXiv:1606.02685 [quant-ph].

[44] G. H. Low and I. L. Chuang, Quantum **3**, 163 (2019), arXiv:1610.06546 [quant-ph].

[45] J. Haah, M. B. Hastings, R. Kothari, and G. H. Low, (2018), 10.1137/18M1231511, arXiv:1801.03922 [quant-ph].

[46] D. W. Berry, G. Ahokas, R. Cleve, and B. C. Sanders, Commun. Math. Phys. **270**, 359 (2007), arXiv:quant-ph/0508139.

[47] R. Babbush, D. W. Berry, J. R. McClean, and H. Neven, npj Quantum Inf. **5**, 92 (2019).

[48] D. Camps and R. Van Beeumen, in *2022 IEEE International Conference on Quantum Computing and Engineering (QCE)* (IEEE, 2022) pp. 104–113.

[49] L. Lin, (2022), arXiv:2201.08309 [quant-ph].

[50] R. Babbush, D. W. Berry, Y. R. Sanders, I. D. Kivlichan, A. Scherer, A. Y. Wei, P. J. Love, and A. Aspuru-Guzik, Quantum Sci. Technol. **3**, 015006 (2017).

[51] W. Kirby, M. Motta, and A. Mezzacapo, Quantum **7**, 1018 (2023), arXiv:2208.00567 [quant-ph].

[52] I. Novikau, E. A. Startsev, and I. Y. Dodin, Phys. Rev. A **105**, 062444 (2022), arXiv:2112.06086 [physics.plasm-ph].

[53] G. H. Low, T. J. Yoder, and I. L. Chuang, Phys. Rev. X **6**, 041067 (2016).

[54] D. Motlagh and N. Wiebe, (2023), arXiv:2308.01501 [quant-ph].

[55] E. H. Lieb and D. W. Robinson, Commun. Math. Phys. **28**, 251 (1972).

[56] L. N. Trefethen, *Approximation Theory and Approximation Practice, Extended Edition* (Society for Industrial and Applied Mathematics, Philadelphia, PA, 2019) https://epubs.siam.org/doi/pdf/10.1137/1.9781611975949.

[57] "Qsppack," `https://github.com/qsppack/QSPPACK`.

[58] V. V. Shende, S. S. Bullock, and I. L. Markov, IEEE Trans. Comput. Aided Design Integr. Circuits Syst. **25**, 1000 (2006).

[59] M. Plesch and v. Brukner, Phys. Rev. A **83**, 032302 (2011).

[60] M. A. Nielsen and I. L. Chuang, *Quantum Computation and Quantum Information* (Cambridge University Press, 2012).

[61] A. Macridin, P. Spentzouris, J. Amundson, and R. Harnik, Phys. Rev. Lett. **121**, 110504 (2018), arXiv:1802.07347 [quant-ph].

[62] A. Macridin, P. Spentzouris, J. Amundson, and R. Harnik, Phys. Rev. A **98**, 042312 (2018), arXiv:1805.09928 [quant-ph].

[63] A. Macridin, A. C. Y. Li, S. Mrenna, and P. Spentzouris, Phys. Rev. A **105**, 052405 (2022), arXiv:2108.10793 [quant-ph].

[64] C. W. Bauer, M. Freytsis, and B. Nachman, Phys. Rev. Lett. **127**, 212001 (2021), arXiv:2102.05044 [hep-ph].

[65] G. K. Brennen, P. Rohde, B. C. Sanders, and S. Singh, Phys. Rev. A **92**, 032315 (2015), arXiv:1412.0750 [quant-ph].

[66] G. H. Low and N. Wiebe, (2018), arXiv:1805.00675 [quant-ph].

[67] M. Kieferová, A. Scherer, and D. W. Berry, Phys. Rev. A **99**, 042314 (2019).

[68] Y. Tong, V. V. Albert, J. R. McClean, J. Preskill, and Y. Su, Quantum **6**, 816 (2022), arXiv:2110.06942 [quant-ph].

[69] L. Lin and Y. Tong, PRX Quantum **3**, 010318 (2022), arXiv:2102.11340 [quant-ph].

[70] D. W. Berry, A. M. Childs, R. Cleve, R. Kothari, and R. D. Somma, Phys. Rev. Lett. **114**, 090502 (2015), arXiv:1412.4687 [quant-ph].

[71] S. B. Bravyi and A. Y. Kitaev, Annals Phys. **298**, 210 (2002), arXiv:quant-ph/0003137.

[72] F. Verstraete and J. I. Cirac, J. Stat. Mech. **0509**, P09012 (2005), arXiv:cond-mat/0508353.

[73] A. Tranter, S. Sofia, J. Seeley, M. Kaicher, J. McClean, R. Babbush, P. V. Coveney, F. Mintert, F. Wilhelm, and P. J. Love, International Journal of Quantum Chemistry **115**, 1431 (2015).

[74] R. Babbush, J. McClean, D. Wecker, A. Aspuru-Guzik, and N. Wiebe, Phys. Rev. A **91**, 022311 (2015).

[75] A. Aspuru-Guzik, P. J. Love, A. Y. Wei, I. D. Kivlichan, D. W. Berry, and R. Babbush, New J. Phys. **18**, 033032 (2016).

[76] K. Setia and J. D. Whitfield, J. Chem. Phys. **148**, 164104 (2018).

[77] W. Kirby, B. Fuller, C. Hadfield, and A. Mezzacapo, PRX Quantum **3**, 020351 (2022), arXiv:2109.14465 [quant-ph].

[78] J. D. Watson, J. Bringewatt, A. F. Shaw, A. M. Childs, A. V. Gorshkov, and Z. Davoudi, (2023), arXiv:2312.05344 [quant-ph].

[79] M. Carena, H. Lamm, Y.-Y. Li, and W. Liu, Phys. Rev. D **104**, 094519 (2021), arXiv:2107.01166 [hep-lat].